Check for updates

Use of some cost-effective technologies for a routine clinical pathology laboratory

Mercedes Vázquez, [iD][a] Laura Anfossi, [iD][b] Hadar Ben-Yoav,[c] Lorena Diéguez, [iD][d] Thomas Karopka,[e] Bartolomeo Della Ventura, [iD][f] Sara Abalde-Cela,[d] Antonio Minopoli, [iD][f] Fabio Di Nardo, [iD][b] Vikas Kumar Shukla, [iD][c] Alexandra Teixeira,[d] Asta Tvarijonaviciute [iD] *[g] and Lorena Franco-Martínez [iD][g]

Classically, the need for highly sophisticated instruments with important economic costs has been a major limiting factor for clinical pathology laboratories, especially in developing countries. With the aim of making clinical pathology more accessible, a wide variety of free or economical technologies have been developed worldwide in the last few years. 3D printing and Arduino approaches can provide up to 94% economical savings in hardware and instrumentation in comparison to commercial alternatives. The vast selection of point-of-care-tests (POCT) currently available also limits the need for specific instruments or personnel, as they can be used almost anywhere and by anyone. Lastly, there are dozens of free and libre digital tools available in health informatics. This review provides an overview of the state-of-the-art on cost-effective alternatives with applications in routine clinical pathology laboratories. In this context, a variety of technologies including 3D printing and Arduino, lateral flow assays, plasmonic biosensors, and microfluidics, as well as laboratory information systems, are discussed. This review aims to serve as an introduction to different technologies that can make clinical pathology more accessible and, therefore, contribute to achieve universal health coverage.

1. Introduction

Clinical pathology is a medical specialty focused on disease diagnosis, prognosis and monitoring, based on the analysis of tissues or biofluids. These analyses include chemistry, microbiology, hematology or molecular pathology tests, among others. They can be applied to various species and sample types, allowing detection of alterations in a wide range of biomarkers and, thus, identifying diseases. For this reason, clinical pathology is a crucial discipline to discern between healthy and diseased individuals, and to perform clinical diagnosis and prognosis judgments, as well as monitoring follow-up and treatment responses.

Clinical pathology laboratories are distributed worldwide and present in almost all hospitals and clinics. However, the need for highly sophisticated instruments that usually have high acquisition and maintenance costs is a major limiting factor, especially in developing countries. The lack of such costly instrumentation may result in poorer patient care, which can be especially detrimental in pandemic times. Another limitation in current clinical pathology laboratories is related to the laborious protocols and manual scoring systems that the pathologist employ, which are in most cases person-dependent and lack reproducible, objective and rapid results, which are crucial for both routine analyses and research studies.[1]

In the last decade, there has been a considerable increase of free and open-source hardware (FOSH) and software (FOSS) in academia, with the growth of articles in this area rising exponentially.[2] The free, open-source (OS) or libre technologies are based on a new, decentralized, participatory and transparent approach for developing software and hardware.[3] These technologies have a series of advantages over traditional products according to Baden *et al.*,[4] including: (1) OS designs are free and developed by users, ensuring suitability for a given task; (2) increased

[a] *National Centre For Sensor Research, School of Chemical Sciences, Dublin City University, Glasnevin, Dublin 9, Ireland*

[b] *Department of Chemistry, University of Turin, Via Giuria, 5, I-10125 Turin, Italy*

[c] *Nanobioelectronics Laboratory (NBEL), Department of Biomedical Engineering, Ilse Katz Institute of Nanoscale Science and Technology, Zlotowski Center for Neuroscience, Ben-Gurion University of the Negev, Beer-Sheva 8410501, Israel*

[d] *Medical Devices Research Group, International Iberian Nanotechnology Laboratory – INL, 4715-330 Braga, Portugal*

[e] *Medfloss.org, Germany*

[f] *Department of Physics "E. Pancini", University of Naples Federico II, Via Cintia 26, I-80126 Napoli, Italy*

[g] *Interdisciplinary Laboratory of Clinical Pathology, Interlab-UMU, Regional Campus of International Excellence 'Campus Mare Nostrum', University of Murcia, 30100 Murcia, Spain. E-mail: asta@um.es*

understanding of the equipment characteristics due to building processes; (3) immediate and local manufacturing; (4) collaboration from experts outside and inside the scientific community. Besides, according to Pearce *et al.*,[5] open-source technologies provided 87% economic savings compared to equivalent or lesser proprietary tools, reaching up to 94% savings when Arduino technology and 3D printing were employed. Therefore, implementing OS resources could be an alternative to expensive commercial solutions or inefficient workarounds such as manual processing in clinical pathology laboratories. For example, economic robots could be made for repeatable laboratory operations such as pipetting, or repositories of mass spectrum sequence fragmentations could be used to validate results and prevent redundant measurements.[6] These actions could lead to significant time and economic savings and wider availability of software and hardware tools for most laboratories.[7] However, OS technologies also present some drawbacks such as the time, equipment, and knowledge needed to create do-it-yourself (DIY) devices, and to achieve quality assurance and reliability for self-built FOSH. Furthermore, although currently there are a vast number of OS digital tools for clinical pathology, including libraries such as OpenSlide (https://openslide.org/) and Bio-Formats (https://www.openmicroscopy.org/bio-formats/), web platforms for data management and collaborative analysis such as Cytomine (https://www.cytomine.org), and software including SlideToolKit,[8] Biii (https://biii.eu/) or QuPath,[1] the field still lacks commonly accepted OS digital tools.[1]

Moreover, the World Health Organization (WHO) recognizes the importance of *in vitro* diagnostics (IVDs) as an essential component to advance universal health coverage, address health emergencies, and promote healthier populations. In this context, the use of point-of-care-tests (POCT) was also recommended in the first edition of the Model List of Essential *In Vitro* Diagnostic (EDL) in 2018[9] and in the 17 Sustainable Development Goals within the 2030 Agenda for sustainable development of the United Nations. These include promoting universal, equitable and inclusive access to health and wellbeing in all ages.[10]

Therefore, the implementation of cost-effective technologies such as 3D-printing and Arduino-based hardware, portable assays, or software solutions can have two order impacts: (1) improved and widen accessibility to various analytical tests, data acquisition, and interpretation, leading to (2) improved health and welfare in subjects and the overall population. Various free and open platforms have emerged to tackle this challenge by promoting support for OS collaboration, development, validation, and dissemination. This review provides the most up-to-date overview on cost-effective and OS hardware and software resources available for the routine clinical pathology laboratory.

2. Open-source lab equipment

One of the most limiting factors for clinical pathology laboratories are the cost of instruments and equipment. In recent years, 3D printing has become a valuable tool for producing low-cost labware in modern research laboratories worldwide, saving hundreds of euros in consumables and simple lab equipment.[11,12] As a fast prototyping technology, 3D printing allows the development and optimization of fit-for-purpose designs in a very short time so that it is possible to test different versions of the prototype quickly during the optimization phase. An extensive selection of hundreds of designs for 3D printing has been made available to the general public through open-source web resources like Thingivers (https://www.thingiverse.com), Instructables (https://www.instructables.com) or the Open-source Lab (https://www.appropedia.org/Open-source_Lab), where users can find and share ready-to-print (.stl) files to 3D print their own lab equipment.

3D printed micropipettes are a clear example of much-needed equipment in every lab that can be printed at significantly lower costs than the commercially available micropipettes. That is probably why it is such a popular part in open-source repositories where a variety of versions can be found, from a simple adjustable-volume straw pipette[13,14] to more sophisticated models.[15–19] An adjustable-volume micropipette suitable for working at 30–300 μL and 100–1000 μL volume ranges was recently printed *via* fused deposition modeling (FDM) and proved to meet ISO standards of accuracy.[19] The full pipette, consisting of the printed parts (the body and the plunger), a disposable syringe, and a few other components, including bolts and nuts, was assembled for a total cost of less than €5 (Table 1). In comparison, adjustable-volume commercial micropipettes will typically exceed €200 on laboratory supplier's websites, although cheaper versions can be found on Amazon.

Stands for holding single[20] or multiple[21,22] micropipettes were also 3D printed *via* FDM. Racks for tubes of different sizes and shapes (including test tubes and centrifuge vials),[23–28] racks for Petri dishes[29] and holders for tubes and beakers[30] have also been commonly produced by 3D printing. Special attention has been received by 3D printed magnetic racks, with final production costs at least 10 times lower than similar commercial magnetic racks, which are rather expensive (*e.g.* magnetic racks for 6–8 × 1.5 mL tubes cost €385 on average in laboratory supplier's websites)[22] (Table 1). Biocompatible well plates were also produced by Selective Laser Sintering (SLS) 3D printing technology using polyamide (PA), a material that can withstand sterilization temperatures.[31] A 3D printed plate adaptor for holding plates over a tablet screen allowed completing complex pipetting patterns by illuminating 96-well or 384-well plates using a tablet computer.[32] This tablet-based tool is part of an open-source project (iPipet) for enabling low-cost liquid handling solutions in high throughput biological experiments (Table 1). Other simple labware 3D printed included origami-inspired forceps,[33] cross tweezers,[34] molds for casting PAGE gels,[35] customizable gel combs[36,37] (Table 1), and microplate flange replacements.[38]

Parts for motorized laboratory equipment have also been commonly 3D printed by FDM. For example, two disc-shaped

Table 1 Costs and cost savings percent associated to building open-source equipment in comparison to equivalent commercial products

Lab equipment	3D printing technology (printer)	OS fabrication costs (€)	Commercial equipment cost (€)	Cost savings (%)	Ref.
Micropipette	FDM	4.13[a]	79–299	95–99	19
Magnetic rack	FDM	~5[a]	60–910	88–99	22
Semi-automated pipetting tool	FDM	128–469[a]	853–1707[a]	73–85	32
Gel comb	MJP	~2	15	87	37
Nutating mixer	FDM	32[a]	318[a]	90	40
8-Channel peristaltic pump	SLA	309[a]	>5120[a]	>94	48
Spectrophotometer	FDM	225	>2300	>90	57

[a] Costs reported in US dollars have been converted to euros for easier comparison (conversion factor, 1US$ = 0.85341 EUR). FDM = Fused deposition modeling; MJP = multi jet printing; SLA = stereolithography.

coverslip holders were printed for integration into an open-source coverslip dryer operated by a 3 V DC motor.[39] A 12 V 25 RPM DC geared motor was used instead to build a 3D printed nutating mixer with a 20° tilt angle platform for gentle agitation of sample tubes of different sizes[40] or for Corning cell culture plates when used with a customized plate holder.[41] The mixer was printed with a low-cost FDM printer using polylactic acid (PLA) for the hard parts and the NinjaFlex elastomer for the flexible parts. The total cost for the fully assembled mixer was €32, saving 90% of the costs incurred when acquiring a commercial nutating mixer with similar capabilities (Table 1). A 3D-printed rotating mixer was built for about the same costs in PLA, and transformed into a mixer-shaker combination with the addition of an Arduino microcontroller.[42] A 12 V DC motor was also used to build a 3D printed centrifuge capable of accommodating six 1.5 mL microcentrifuge tubes and fitted with a safety lid.[43] Another version incorporated a 1806/2400 brushless DC motor taken from a drone controlled with the help of an electronic speed controller (ESC) and an Arduino Nano.[44] A simpler design was employed to construct a centrifuge capable of spinning at up to 33 000 rpm, where a rotor for holding six Eppendorf tubes was 3D printed and attached to a Dremel rotary center.[45] Although this system allowed operation within ultracentrifuge regimes, no safety enclosure was integrated and so maximum caution needed to be exercised when operating this system. An open-source homogenizer consisting of a 3D printed sample tube holder connected to a reciprocating motor *via* a chuck adapter was also developed to work with 2 mL conical sample tubes[35] (Table 1). Two different configurations for accommodating two or six sample tubes simultaneously were successfully tested for preparation of DNA modified hydrogel particles by dispersion polymerization. Parts for building an open-source magnetic stirrer were also 3D printed and assembled to fit two strong magnets and a standard 80 × 80 mm computer fan, whose rotation speed was controlled either *via* a potentiometer[46] or a multi-voltage power adapter.[47] The development of a peristaltic pump for handling sample volumes in the microliter range has also been possible through 3D printing technology.[48] The pump parts were printed *via* stereolithography (SLA) to ensure the mechanical strength

and accurate reproduction of the parts required for this application. The printed parts were easily assembled together with a stepper motor, and a few other off-the-shelf parts, to produce a pump with 8 channels delivering flow rates in the range 0.7–5750 μL min⁻¹ when run by the stepper motor software. In comparison to commercial 8-channel peristaltic pumps, the open-source pump was much smaller and about 17× times cheaper, with a final cost of about €300 (Table 1).

Optical lab equipment is another area that has been increasingly explored by 3D printing users - from simple stands allowing quick and precise focusing of low-cost commercial USB microscopes[49,50] to fabrication of open-source microscopes from scratch,[51] including the corresponding smartphone adapters for the acquisition of digital photos.[12,52,53] A really simple microscope based on a 3D printed clip to insert a glass sphere and easily connect with a smartphone was also fabricated for under €1.[54] Different models of smartphone-based spectrometers have also been made available through open-source resources over the years. Those typically integrate a commercial diffraction grating (or a piece of a DVD-R disc acting as such[55]) within the spectrometer body that can be entirely 3D printed.[56] Miniature spectrophotometers have also been developed within the open-source communities with the aim of low cost and portability in mind. A recent example of those open-source spectrophotometers consisting of an LED, a mini spectrometer, an Arduino microcontroller, and a Bluetooth module was fabricated for only €225 (ref. 57) (Table 1). The casing to fit all these components was 3D printed by FDM using a black thermoplastic to minimize light reflection within the system. The 3D printing case integrated a cuvette holder for a standard off-the-shelf cuvette covered with a black lid for measurements. Data was transferred to a mobile application *via* Bluetooth.

Applications of 3D printing in cell culture operations have also resulted in creative open-source solutions that improve the control of the experimental conditions. For example, a 24-well plate insert for oxygen control in cell culture studies was 3D printed by SLA.[58] The insert network sat on top of a gas-permeable layer of polydimethylsiloxane (PDMS) and allowed gas distribution to four rows of six wells independently, so that four different oxygen conditions could

be controlled simultaneously. SLA was also used for printing a shaking flask lid for application in the cultivation of bacterial cells.[37] The lid integrated Luer connectors and tube adapters that allowed both sampling and feeding without process disruption.

In this section, cost-effective approaches to hardware development have been revised. These methodologies allowed reducing cost for sample preparation before analysis, posing up to >99% economic savings in clinical pathology laboratories. Similarly, the next part will revise portable, economical methods that eliminate the need for specific instruments and trained personnel and improve clinical pathology by making it more accessible.

3. Portable assays

The 'no one must be left behind' principle in the health field means guaranteeing universal health coverage and access to quality health care. To that end, the use of POCT is particularly beneficial in developing countries to strengthen their capacity for early warning, risk reduction, and management of national and global health risks. However, POCT are also of great benefit for clinical pathology worldwide due to their essential advantages over non-portable assays. For example, the study of dysfunction or deregulation of metabolites, proteins, transcriptional factors, genes, and metabolic pathways with POCT makes rapid and robust diagnosis using low sample and reagent volumes.[59–62] Moreover, integration of immunoassays,[63] magnetic separation techniques,[64] and spectroscopic[65] and electrochemical[66] techniques with POC devices can significantly improve the on-site analysis capacity (portability), ease-of-use, sensitivity, specificity, and sample-to-answer diagnostics.[67] Therefore, these biomedical microsystems have revolutionized clinical pathology, such as the creation of portable pregnancy test or glucometers that can be easily utilized by the final user. Different economical approaches for production of portable assays and POCT that can be used as economical alternatives in clinical pathology laboratories will be discussed in the following subsections.

3.1. Lateral flow assays

The lateral flow assay (LFA) is a paper-based (bio)analytical technique for the on-site detection of target molecules, where the sample is added on a standalone device, and the result is obtained in a few minutes. LFAs are one of the most successful and widespread POCT currently available due to their rapidity, affordability, and simplicity. These tests can be performed and results interpreted just by following the manufacturer's instructions without needing special instrumentation, infrastructure or expertise in the technique. However, it is not unusual that LFAs are recommended for health care facilities with clinical laboratories since their use can help reduce the workload, optimize treatment decision-making, avoid referrals, and improve clinical care and patient

outcomes while decreasing costs. This is quite in agreement with the widespread use of lateral flow immuno assays (LFIA) (*i.e.* LFAs in which the recognition element is usually an antibody) in developed countries, which represent the most profitable market for the LFA manufacturers.[68]

In brief, LFAs rely on capillary forces to move the liquid sample and a suitable labeled recognition element along overlapped and sequential porous materials (Fig. 1). The sample migrates from the conjugate pad which releases the labeled recognition element (usually an antibody in LFIA) leading to an analyte-recognition element interaction (usually an antibody–antigen interaction). Generally, gold nanoparticles and latex particles that produce a colored readout are used as labels. Next, the sample and the labeled recognition element reach the analytical porous membrane that contains bioreagents (mostly antibodies or analyte analogue) immobilized on the so-called Test line and Control line to complete the analyte detection and ensure the correct functioning of the test. Finally, the sample ends its run into the absorbent pad.

A typical LFIA device will therefore consists of four fundamental components laminated on a backing card for better handling (Fig. 1): (i) a sample pad (typically of cellulose) with the role of helping and controlling the distribution of the sample onto the conjugate pad; (ii) a conjugate pad (typically of glass fiber or polyester) that will hold the labeled recognition element in a dry state, maintaining it stable over the entire shelf-life (in some cases up to 2 years) and releasing it efficiently, uniformly, and reproducibly when the assay is run; (iii) a porous membrane, generally nitrocellulose, being probably the most critical component and the analytical region of the device, aiming to bind proteins in well-defined areas (*i.e.* test and control lines); (iv) an absorbent pad of high-density cellulose that enhances the capillary driving force and absorbs all the unreacted substances that can potentially cause nonspecific and misleading signals, and decreases the signal background. In addition, the strip can be placed into a plastic cassette that applies pressure where the different components overlap, making the flow uniform, increasing the robustness of the system, and protecting the test strip. The traditional plastic cassettes are usually very cheap (*ca.* €0.04 per unit or less). Nevertheless, new tests may require different cassette design to fit a particular strip design. In this sense, 3D printing would be the best approach to evaluate several custom configurations at a low cost. However, to the best of our knowledge, no open-access designs for 3D printing of LFIA cassettes are yet available.

Although the fabrication of the LFIA strips is easy and simple, the process involves dispensing of (bio)reagents that typically requires expensive instruments, which can cost tens of thousands of euros because of the complexities arising from their ability to dispense or spray small amount of reagents, and the ability to precisely control the dispenser head's position.[69] The investment in traditional dispenser can be easily amortized for companies that produced a huge
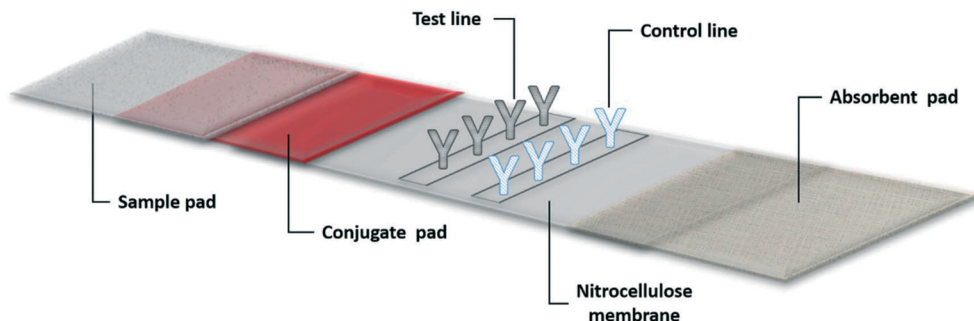
Fig. 1 The scheme of a typical LFIA strip.

amount of strips. Nevertheless, the replacement parts are still quite expensive. Therefore, a cheaper alternative would be highly valued. Currently, these cost-effective dispensing alternatives are mainly useful in small scale-experiment, feasibility test and concept validation. Some examples have been reported in the literature with the aim to replace these expensive dispensers. For example, Choi et al. demonstrated the use of a fountain pen dispenser consisting in a moving pen holder, a holder supporting part and a fountain pen to draw the Test and the Control lines, loading the reagent solution into the ink reservoir, as with conventional ink.[70] Credou et al. reported the use of a commercially available inkjet printer to print antibody solutions on a cellulose substrate.[71] Most recently, Han and Shin proposed a low cost, 3D printed open-source reagent dispenser that can be easily built and used for drawing the test and the control lines.[69] For easy replication of the open-source device, the authors used the Arduino Uno to control the dispenser. The dispensing head was a syringe needle, which is commercially available, and can be easily attached and detached from the needle holder.

LFIA formats are either immunometric (also known as sandwich or direct assay) or competitive (competitive inhibition), depending on the type of target analyte and antibodies binding sites occupancy. Immunometric immunoassays rely on direct measurement of occupied "capture-antibody" binding sites using, for example, a second labeled antibody directed against occupied sites. Conversely, the competitive immunoassays rely on indirect determination of binding site occupancy by measurement of unoccupied sites using, for example, a labeled analyte or an analyte analogue.[72]

By shortening the time to result, the use of LFIA in the management of diseases offers several benefits, e.g., starting immediately an adequate treatment and, thus, reducing the incidence of complications. For example, LFIA can help distinguishing between bacterial and viral infections, identifying cases where antibiotics therapy is needed, limiting the overuse of drugs that lead to accelerate the antibiotic resistance. Moreover, a rapid identification of an infected person allows limiting the infection spread itself, helps clinician to make the right decision in a timely manner, as well as reduces unnecessary costs for the health care systems and/or for the patients.

It is not by chance that LFIA peculiarities made them one of the ideal POCT to be used in low-resource field environments and in developing countries that cannot afford standard analytical instrumentation to perform analyses. The WHO EDL recommend LFIAs for use in community settings and health facilities without laboratories, including health posts and centers, doctors' offices, outreach clinics, ambulatory care, and home-based and self-testing, being listed for pregnancy testing, cholera*, cryptococcal meningitis, hepatitis B and C, HIV, influenza A and B*, malaria, syphilis, tuberculosis, and visceral leishmaniasis* (* added in 2019[73]). Nevertheless, the LFIA use in clinical laboratories is somehow recommended since they are also listed in the EDL for health care facilities with clinical laboratories, including district, regional, provincial or specialized hospitals or laboratories and national reference laboratories. In this setting, LFIAs for the detection of C-reactive protein, dengue virus*, and procalcitonin are reported, in addition to those already mentioned for use in community settings and health facilities without laboratories (* added in 2019[73]).

Despite the potential benefits, the WHO recommendation (not prescriptive), and the plethora of LFIA reported in the literature and commercially available, the routinely use of LFIAs in clinical pathology laboratory is not well-documented. The reasons for this discrepancy may be various, starting from the LFIAs inherently suitability for use outside the laboratory setting, especially as self-tests (being the pregnancy test the most striking example). Other main reasons may be: a) the lower reliability in comparison to traditional laboratory-based techniques; b) the need of confirmatory analysis usually for LFIAs positive results; c) the impossibility to obtain quantitative results; d) possibility of errors in subjective interpretation and transcription; e) lack in results traceability; f) the need to be listed in national or international guidelines in order to be effectively used; g) the limited reimbursements for LFIA devices; h) lack in information regarding the devices, aimed at assessing their actual implementation benefits. However, some of these issues can be solved thanks to the use of strip readers in a handheld or bench format with integrated features that, in addition to results quantification, allow data digitalization, tracking, storage, and transmission, reducing interpretation

and transcription errors, and thus ensuring testing quality and control. The use of LFIA readers has been considered as a weakness in low-resource settings, mainly because it increases the cost per analysis. However, it would represent an advantage for clinical laboratories that currently rely on high cost and highly complex analyzers that also require high maintenance costs.

In recent years, the idea of employing a smartphone camera as an optical sensor and performing digital image processing on the phone has become quite popular.[74–76] Moreover, the use of an external high-sensitive optical detector which is attachable to the smartphone through its communication ports (*e.g.*, audio jack, USB port, Bluetooth) instead of using the phone's inbuilt sensors, has been also exploited.[75] Within this context, some economical open-source readers have been recently proposed specifically for LFIAs. For example, Parra *et al.* developed an automatic lateral flow-based test reader using a Raspberry Pi single-board computer and open-source software frameworks to provide real-time image collection and processing.[77] Images and results were displayed on a Raspberry Pi 7″ touchscreen display and the whole system was powered by a 6.4 V rechargeable battery. The reader acquired and analyzed images of LFIAs with the same contrast and accuracy as a standard flatbed high-resolution scanner coupled to a laptop computer, for less than one-fifth of the cost. Huttunen *et al.* even developed a €100 portable device for measuring fluorescence signals from a LFIA strip.[78] The proposed device was capable of exciting fluorescent labels with 532 nm and 650 nm lasers and collecting the emitted fluorescent light with a camera. The core of the device was a Raspberry Pi Zero W wireless single-board computer that controlled the Raspberry Pi camera v2 module and the lasers. The computer could also perform the image analysis and communicate the results to a mobile phone application acting as a user interface. The whole system was powered through a micro-USB charger or a lithium-ion battery, and custom Python 3 scripts were used to control the camera and lasers.

3.2. (Direct) detection of infective agents by plasmonic biosensors

Optical biosensors relying on microplate-based methods are the most commonly used for POCT and high-throughput assays.[79–81] In fact, ELISA still represents one of the gold standards in clinical trials. Nevertheless, the high costs and time consumption are continuously spurring the researchers to go beyond such colorimetric assays based on enzymatic reaction. In this regards, the so-called plasmonic-ELISAs tend to reduce the kit costs while preserving or even improving the sensing performance.[82] Despite the remarkable outcomes and possibility to retrieve a visual response, it usually seems to be not apt to provide a quantitative result.[83]

Fluorescence readouts might constitute a possible way to combine the reliability with accuracy in quantifying the target concentration. Moreover, the opportunity to augment the fluorescence *via* plasmon-enhanced fluorescence (PEF) is of relevance in bioanalytics since it could pave the way to development of ultrasensitive and high-throughput assays.

In addition, the development of the cost-effective bottom-up nanotechnologies contributes to fill the gap between the material fabrication and their applications, being high-sensitive biosensing one of the most prominent fields of application.

So far, three known mechanisms have been ascertained to contribute to the PEF effect: (i) modification of the fluorophore excitation rate, (ii) modification of the fluorophore radiative decay rate (Purcell effect), (iii) energy transfer quenching to the nearby metal.[84] All of them are depicted in Fig. 2. The spectral overlap between the plasmon extinction and the fluorophore excitation or emission determines whether Förster resonance energy transfer (FRET) or Purcell effect is predominant.[85] If the plasmon overlaps with the fluorophore excitation, the rate of the latter is enhanced through the FRET mechanism at separation distances of a few nanometers due to the presence of the intense near-field (E_p) of the plasmon (Fig. 2a and d).[85] On the contrary, the overlap of the plasmon with the fluorophore emission provides a large fluorescence enhancement through the Purcell effect for separation distances beyond the FRET region while a progressive decrease of the radiative rate occurring at smaller distances due to the increasing quenching *via* non-radiative losses into the metal nanostructure (Fig. 2b and d).[85]

Although the plasmon could re-radiate the stored energy enhancing the emission intensity, the near field of the dipole also excites higher non-radiative order modes in the plasmon preventing the re-radiation of this energy into the far field, leading to an overall quenching at separation distances of a few nanometers.[85] It is usually unfeasible to obtain a pure excitation or emission enhancement due to the limited Stoke shift of the fluorophore and the relatively broad extinction line width of the plasmon (Fig. 2c). Thus, a balance of both mechanisms takes place yielding the so-called dual-mechanism enhancement.[86] In such a case, an intense fluorescence enhancement arises at an optimal distance of ~10–15 nm, a strong quenching being present at shorter separation distances, whereas a return to the no enhanced fluorescence conditions occurs at longer distances due to the weaker plasmon-fluorophore coupling (Fig. 3d).[85]

As examples of the potential usefulness for plasmonic biosensors in clinical pathology laboratories, their application to the diagnosis of malaria *Plasmodium falciparum* lactate dehydrogenase (*Pf*LDH), a malaria biomarker,[87] and the virus SARS-CoV-2 that is causing one of the broadest pandemic of the last decades, is briefly described below.

*Pf*LDH is present at nanomolar level in red blood cells but only at picomolar levels in the serum of infected people. PEF-based devices, in combination with a unique biofunctionalization procedure based on the well-established photochemical immobilization technique (PIT), led to
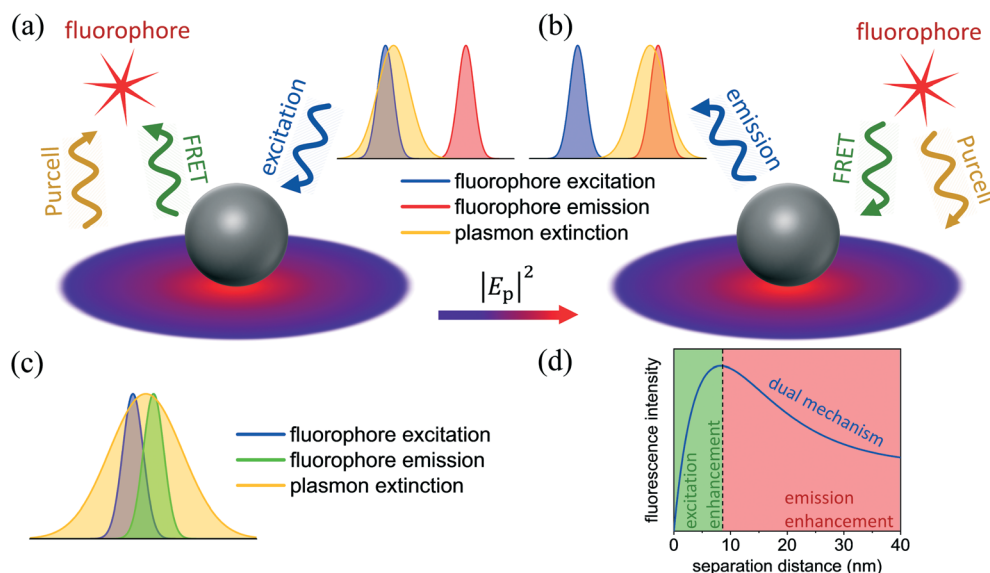
Fig. 2 (a) Excitation mode enhancement through either FRET or Purcell effect due to the spectral overlap between the plasmon extinction and the fluorophore excitation. (b) Emission mode enhancement through either FRET or Purcell effect due to the spectral overlap between the plasmon extinction and the fluorophore emission. (c) If the plasmon extinction encompasses both the excitation and emission peak of the fluorophore, a dual-mechanism enhancement takes place. (d) Fluorescence enhancement mechanism as a function of the nanostructure-fluorophore separation distance.

immunosensors suitable for detecting *Pf*LDH at femtomolar level in whole blood.[88,89] PIT allowed the effective tethering of antibodies with the right orientation directly onto gold surfaces in only a few minutes by using a simple UV lamp.[90] The detection scheme is reported in Fig. 3a together with the signal detected at a *Pf*LDH concentration of 100 nM (Fig. 3b) corresponding to 14 μg mL^{-1} (*Pf*LDH molecular weight is 140 kDa). The comparison with the image detected when no target was spiked in the human blood (control) shows a noticeable difference that suggests a wide detection range.

This is visible in Fig. 3c (dose–response curve) from which a limit of detection based on the 3 times the standard deviation (SD) criterion provides approximately 25 fM (3.5 pg mL^{-1}). It is worth mentioning that the transduction mechanism (Fig. 3a) does not rely on mass, but rather on the molar concentration. It is expected that the molar limit of detection will be kept even when this biosensor is applied to lighter analytes thereby pushing the mass limit of detection in the range of fg mL^{-1}. This is even truer if we consider that the original blood sample, although not treated, was diluted
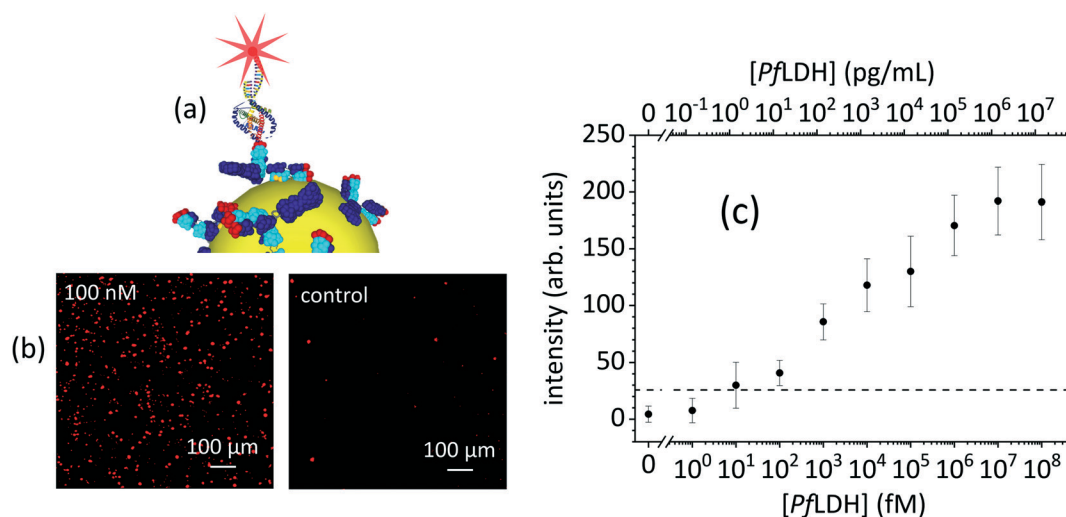

Fig. 3 (a) Sandwich detection: antibodies (immunoglobulin G, IgG) are tethered to the gold nanoparticles (AuNPs) by PIT and bind *Pf*LDH that is recognized from the top by an aptamer tagged with a fluorophore. (b) Images of the substrate recorded at a *Pf*LDH concentration of 100 nM (14 μg mL^{-1}) and without *Pf*LDH (control), respectively. (c) The intensity shown in panel (b) is reported *versus* *Pf*LDH molar and mass concentration (bottom and top scale, respectively). The horizontal line represents the threshold for a detectable signal (LOD) [adapted from ref. 89].

1 : 100 due to its opacity. Thus, an improvement of two orders of magnitude is expected when transparent matrices are analyzed (*e.g.* serum). This technology could be easily implemented in a 96-well plate at a total cost of approximately €10. The reading time could be of the order of few minutes by using a multiplate reader.

Although quantitative detection is generally required, in many applications the detection by naked eye is preferred. Additionally, a visual response seems to be perfectly suitable for detecting analytes in laboratories with fewer resources and time constraint. In particular, it is even more evident during the current pandemics in which reliable visual and rapid POCTs against SARS-CoV-2 significantly help to reduce the spreading of the infection. As a matter of fact, since the COVID-19 pandemic started last year, mass testing has been fundamental to identify and isolate clusters in an effort to limit and eventually eradicate SARS-CoV-2.[91] The gold standard for diagnosing COVID-19 infection (*i.e.* reverse transcription real-time polymerase chain reaction – rtPCR)[92] is able to detect the virus genetic material (RNA) in samples collected *via* a naso-oropharyngeal swab, but due to its complexity, it can hardly be appropriate for mass screening.[93–95] As a simpler, faster and cheaper alternative, a colorimetric biosensor based on metal nanoparticles was recently presented for SARS-CoV-2 detection, exhibiting a limit of detection close to that of rtPCR.[96] This kind of biosensors present unique optical properties, which makes them highly suitable for development of easy-to-use and

rapid colorimetric diagnostic tests for POCT or even for home use. This approach relying on nanoparticle aggregation induced by the presence of an antigen was also used to detect the influenza A virus, but no clinical application was reported to demonstrate the effectiveness of the whole procedure in clinical cases.[97]

The effective surface functionalization of the colorimetric biosensor for SARS-CoV-2 detection was again done *via* PIT resulting in a biosensor that can be used for COVID-19 mass testing with >95% sensitivity and specificity.[96] The detection scheme is shown in Fig. 4 and consists of a red colloidal solution of 20 nm diameter gold nanoparticles (AuNPs) PIT-functionalized against three surface proteins of SARS-CoV-2: spike, envelope and membrane. In this approach, the sample – consisting of untreated naso-oropharyngeal swab specimens – was mixed with the functionalized AuNPs and the optical response of the solution was measured for evaluating the presence of SARS-CoV-2. The presence of the viral particles (virions) in the sample induced the formation of a nanoparticle layer on its surface (Fig. 4b) that led to a redshift (from 525 nm to 560 nm) of the optical density (OD) in the extinction spectrum of the solution, being visible even by naked eye (change of color from red to purple) if the viral load was relatively high. Moreover, the optical density measurement was performed at a single wavelength (560 nm) to allow using a simple colorimeter to carry out the measurements. To achieve a high-throughput screening, the reading could be performed in 96-well plate (Fig. 4c) by using a commercial multiplate
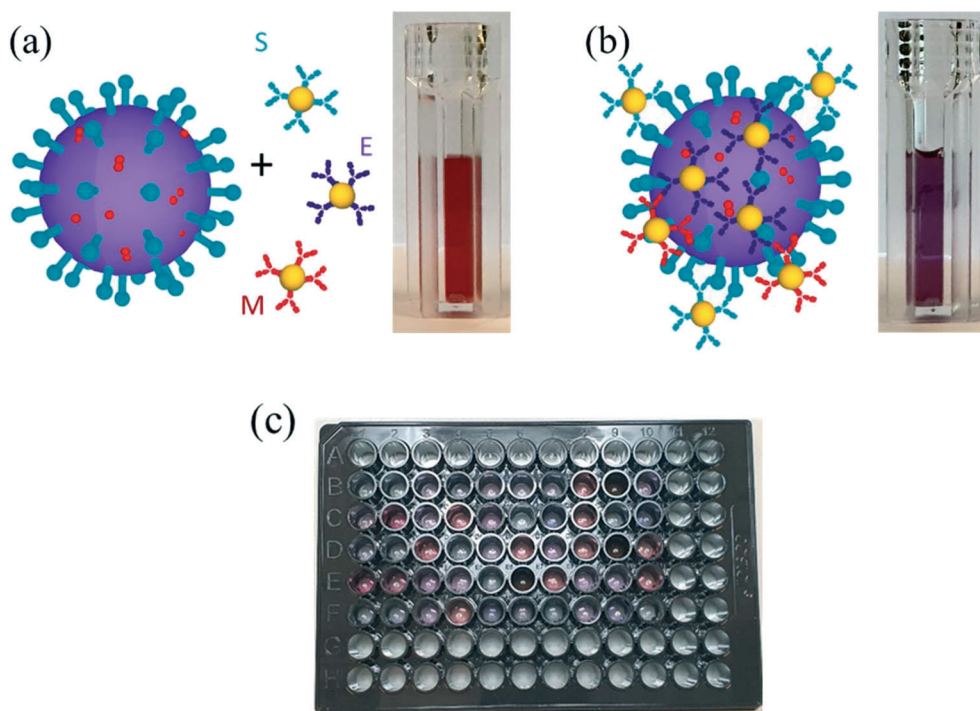

Fig. 4 Principle of the colorimetric biosensor for SARS-CoV-2. (a) AuNPs are functionalized to target SARS-CoV-2 proteins (spike (S), envelope (E), and membrane (M)). The picture shows the pink colloidal solution containing the functionalized AuNPs. (b) The functionalized AuNPs surround the virion forming a nanoparticle layer on its surface that leads to a color change visible in the picture. (c) Picture of the 96 multiwell plate containing 250 μL of positive samples [adapted from ref. 96].

reader within a few minutes. The cost of each test could be estimated at less than €1.

3.3. Microfluidic devices

Microfluidics consists on the study and manipulation of fluids flowing through a micro channel. In recent years, microfluidic technology has been the subject of great interest from the scientific community due to its potential for miniaturization, automation, integration, and high throughput that allows the handling of small volumes of samples and reagents, with operational fidelity, reduced sizes, and cost-efficiency.[98–100] For the fabrication of microfluidic platforms nowadays, 3D printing techniques are the most demanded, although other unconventional approaches including soft lithography using 3D printed molds,[101] printed circuit board (PCB) methods,[102] xurography[103] and paper-based methodologies,[104] are also good low-cost alternatives. The application of microfluidic devices into health monitoring and clinical pathology will be discussed in the following subsections.

3.3.1. Lab-on-chip multiomics for health monitoring. Lab-on-chip (LOC) devices have made a significant impact in the health sciences field in the last decades, particularly through the integration of bioassays into microfluidic devices for POCT applications in rapid and real-time diagnosis, detection and monitoring of diseases. The monitoring of human metabolomics, proteomics, and genomics using microfluidic-

based LOC devices is a more cost-effective approach than traditional lab-based methods which require many pre-treatment steps, high cost instruments, and the need of skilled personnel to operate those.

The metabolome is the collection of small biomolecules in metabolic pathways of humans; these biomolecules are known as metabolites. Alterations in the levels of metabolites in any of the metabolic pathways (https://hmdb.ca/pathways) may refer to a particular disease. For instance, the change in levels of cortisol,[105] phenylalanine,[106] uric acid and creatinine,[107] glucose and lactate[108,109] can indicate mental illnesses, phenylketonuria, renal function, exercise intensity, and diabetes mellitus, respectively. Glucose was detected in saliva using a novel LOC device integrating an optical sensor[108] (Fig. 5a). This device was divided into three parts: (1) a pretreatment area, where H_2O_2 was produced via chemical reaction between glucose and glucose oxidase; (2) a mixing area, where the resulting H_2O_2 was mixed with a colorimetric reagent (N,N'-diethyl-p-phenylenediamine, 4-chloro-1-naphthol and horseradish peroxidase) via obstacles embedded in the microchannels; (3) a measurement area, where absorbance measurements were taken with a photodiode following blue color development in the presence of H_2O_2. This low-cost LOC was presented as a highly sensitive, non-invasive, portable device suitable for diabetic patients. For detection of cortisol in saliva, Vinitha et al. presented a polymer-based LOC based on a microfluidic capillary flow assay (MCFA) with on-chip dried reagents and
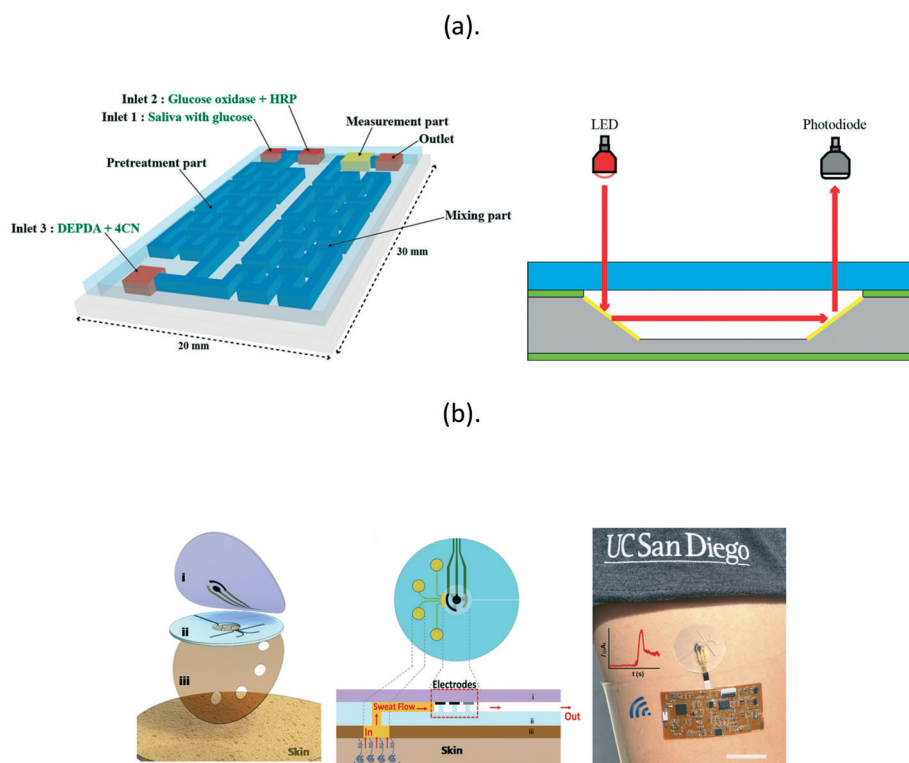
(a).

(b).

Fig. 5 LOC based platform for metabolites detection. (a) LOC optical sensor. Integrating an 45° etched reflective surface for increased optical path length in absorbance measurements of glucose in saliva;[108] (b) epidermal electrochemical microchip for detection of lactate and glucose in sweat.[109]

integrated with a portable fluorescence analyzer.[105] This approach could be also very promising for the analysis of blood, serum, and sweat samples. Finally, a skin-mounted microanalytical flow system with embedded electrochemical detectors was fabricated for continuous real-time monitoring of glucose and lactate in sweat.[109] This device consisted of three layers of polydimethylsiloxane (PDMS): the first layer of PDMS incorporated three microelectrodes, *i.e.*, reference (RE), working (WE) and counter electrodes (CE); the second layer embedded the microchannels for flow and analysis of samples; and the third layer allowed adhesion to the skin and helped to collect proper sweat samples (Fig. 5b). The simultaneous analysis of multiple analytes provides more suitable and trustworthy information compared to the monitoring of a single metabolite, thus, it is highly desirable in personalized monitoring applications. In conclusion, there are a variety of novel and cost-effective microfluidic devices for the monitoring of human metabolites already paving the way for low-cost health monitoring with the incorporation of miniaturized, non-invasive, and robust LOC, as those presented above.

In proteomics, biomarker proteins have been used for the prognosis and diagnosis of different diseases. The detection process of these proteins usually involves high-demanding assays in terms of costs, instrumentation and specialized personnel. In contrast, Chiadò *et al.* developed a 3D printed LOC for the detection of protein biomarkers such as vascular endothelial growth factor and angiopoietin-2, which is responsible for angiogenesis and plays important role in breast cancer and metastasis[110] (Fig. 6a). The developed device was fabricated using 3D-digital light printing (DLP) SLA to produce polymeric platforms. 3D printing offered a high degree of scalability of the device due to its cost-effectiveness. Moreover, for the detection, the immobilization of the biorecognition element which is anti-ang-2-antibody was carried out by the addition of acrylic acid in the polymer to introduce the controlled carboxylic acid (–COOH) groups. Thereby, the immobilization of bio receptors was performed *via* covalent bonding between the COOH group and the antibody. Balakrishnan *et al.* used lithographic methods for the development of polysilicon nanogap (PSNG) electrodes onto an LOC for the detection of human chorionic gonadotropin (hCG), which is very beneficial for the health monitoring of pregnant women as well as an essential biomarker for the many malignant cancers, ectopic pregnancy, and chorioepithelioma.[111] The non-bio-compatible structure of PSNG electrodes was initially modified with hydroxyl groups using the Fenton reaction, and was then attached to silane *via* the –OH groups, resulting in an amine-terminated surface. The subsequent
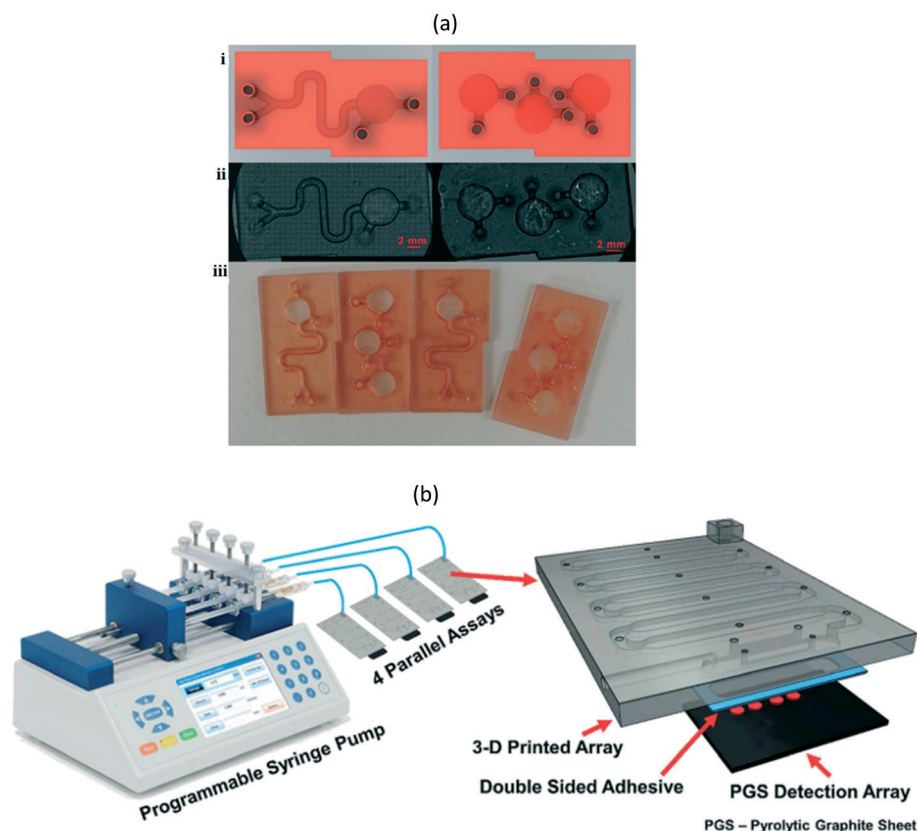

Fig. 6 (a) (i) CAD of two different LOC devices; (ii) microscope images of the 3D printed microfluidic devices; (iii) images of the printed modular chips.[110] (b) Programmable pump configured for four parallel immunoassays on microfluidic immunoarrays (left) and a model of the compact 3D-printed immunoarray (right) attached to a pyrolytic graphite sheet (PGS) 4-microwell detection array.[112]

immobilization of hCGab resulted in a surface ready to detect the hCG biomarker. Simultaneous analyses of four serum samples for detection of prostate-specific antigen (PSA) and prostate-specific membrane antigen (PSMA) in the diagnosis of prostate cancer and its metastases was also possible using 3D printed microfluidic devices[112] (Fig. 6b). For the detection, the 3D printed electrochemiluminescent immunoarray was integrated with nanostructured graphite sheets with inbuilt microwells. The four simultaneous measurements could be performed in less than 20 min using 1–2 μl sample volume.[112] A total assay cost of €0.64 showed promising potential in the clinical health monitoring. Finally, Kadimisetty et al.[113] also developed a 3D-printed automated immunoarray capable of simultaneous electrochemiluminescent detection of 8 proteins that could act as biomarkers of prostate cancer in human serum. The works above have shown the potential of proteomics detection for the diagnosis of malignant diseases.

LOC devices also represent a feasible economic alternative to conventional enzyme-linked immunosorbent assays (ELISA), polymerase chain reaction (PCR), and cell culturing methods used in genomics. For example, Zika virus RNA was recently analyzed using smartphone detection following loop-mediated isothermal amplification on paper microfluidic chips.[114] Cai et al. also detected MicroRNAs (miRNAs) of cancer cells using a paper-based laser-induced fluorescence (LIF) microfluidic assay with the addition of duplex-specific nuclease (Fig. 7).[115] Two specific probes were kept on the paper-based chip inside 4 mm diameter circles. When the miRNAs were added, the reaction enabled amplification of the fluorescence signal. The paper-based device showed good results with cancer cells of HeLa and A549 in a total assay time of 40 min. Nestorova et al. developed a DNA-based biosensor in integration with a thin film of antimony/bismuth thermopile introduced into the lower channel wall of a microfluidic device for the measurement of heat produced changes up to order of 10^{-4} K during the DNA hybridization reactions.[116] This concept was further extended to study the nucleic acid sequences and it was observed that the thermometric LOC successfully distinguished the complimentary and non-complimentary sequences of nucleic acid, besides gene expression analysis, genetic mutations,

genotype, and many pathogen detections. Lastly, Kaprou et al. presented a platform of fast DNA amplification based on helicase-dependent amplification that was exploited for the detection of mutations related to breast cancer and salmonella. This device amplified the DNA of exon 20 of the BRCA 1 gene which contains two positions where significant mutations occur.[117]

Overall, although LOC devices have shown promising results term of sensitivity, low limits of detection (LOD), reproducibility and specificity, new approaches based on semi-selective arrays of electrodes in combination with machine learning methods could be really helpful in overcoming the challenge of multiplex detection for monitoring of metabolic pathways.[118] In addition, machine-learning algorithms and artificial intelligence can enhance the diagnostic ability up to around 90% to 95%,[119] allowing earlier detection of illnesses with increased sensitivity, specificity and accuracy.

3.3.2. Microfluidics for whole cell analysis. The development of microfluidics has led to significant improvements in many diagnostic areas in recent years, leading to a more accurate and rapid diagnosis compared with standard tools.[99,120,121] Many standard laboratory procedures can be adapted to be implemented in disposable microfluidic cartridges for smooth and efficient operation, yielding minimal inter-user or inter-laboratory variability. Therefore, microfluidics has the potential to be used as a complementary technology, or even as a replacement, for clinical pathology operations.

The application of microfluidics in the separation and analysis of blood components brings several advantages in comparison to manual cell enumeration or modern cytometers, starting from the miniaturization of large conventional equipment, reduced reagents and sample volume lowering the cost per test, and since microfluidic chips are disposable, there is no need to use reagents for system cleaning avoiding potential sample contamination. Standard flow cytometry assays can cost up to €100 per test to analyse small volumes of sample (50 μL) and taking up to 3 hours, using several hundreds of microliters of expensive antibodies.[122] On the other hand, microfluidic chips for cell sorting can be as cheap as €1–10 per test, and are able to
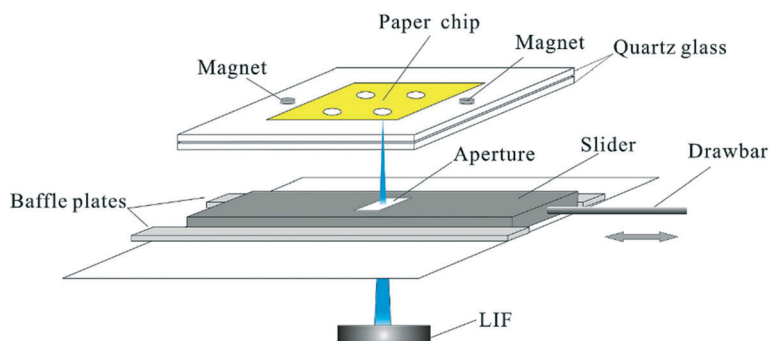

Fig. 7 The diagram of the interface for LIF detection.[115]

process several mL of sample in less than 1 h with internal volumes lower than 50 μL, saving dramatically on reagent costs.[123]

For hematology, modern cytometers are very expensive, need to be operated by trained personnel, and require high volume samples, drawbacks that can be solved with microfluidics. In clinical microbiology, the ability to couple microfluidic chips with several other detection techniques[124] such as mass spectrometry,[125] fluorescence spectroscopy,[126,127] electrochemistry,[128] loop mediated isothermal amplification (LAMP),[129,130] or PCR[129] for the analysis of microorganisms, was also demonstrated. Similarly, microfluidic platforms boomed in the past decade also in the reproductive biology,[131,132] having been applied as sample processing elements, analytical platforms, and supporting more complex operations, even a menstrual cycle and a human reproductive tract[133] (Fig. 8D). In the case of histology and cytology, since microfluidics promotes multiple assays at the same time in a very reduced single tissue section, the application of several techniques together – microfluidics, stains and immunohistochemistry – allows to obtain a more accurate and complete diagnosis, especially in clinically rare and difficult samples.[134]

Examples of application of microfluidics in hematology, clinical microbiology, histology and cytology are summarized in Table 2. Overall, these technologies hold great potential towards accessible, less costly and time-consuming alternatives.

4. Open-source laboratory information systems

Regardless if they are more focus on clinical medicine or research, clinical pathology laboratories usually cope with large amounts of data that need specific digital tools to be managed. Free/libre and open-source software (FLOSS) has a long history in health informatics. The VistA software of the Veterans Health Administration in the US is more than 35 years old and is running in many hospitals around the world, as well as its derivatives from OSEHRA (https://www.hardhats.org/) and WorldVista (https://worldvista.org/). Many other systems including complete hospital information like GNU Health (https://www.gnuhealth.org/), medical record systems like OpenMRS (https://openmrs.org/), and DICOM servers like ORTHANC (https://www.orthanc-server.com/), are now offering flexible and cost-effective alternatives to proprietary software products. Also, in the domain of laboratory information systems (LIMS) there are dozens of free alternatives available which will be presented in this section.

The term FLOSS is a combination of Free/Libre Software and open-source Software, two principles that have the same roots, but have certain differences. The term "libre" refers to
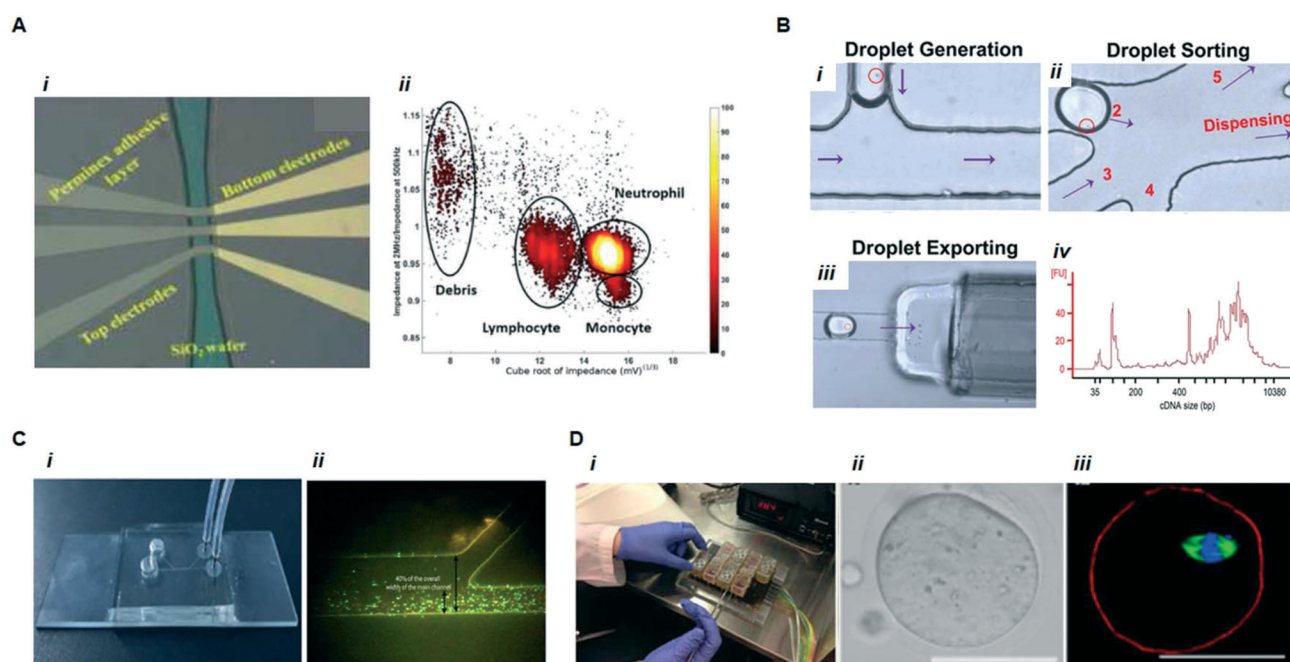

Fig. 8 Representation of different microfluidic platforms for distinct applications. A) Portable instrument for complete blood count hematology: i) image of the impedance sensor showing bonded wafer, fluidic channel and diced chip; ii) cell discrimination through a scatter plot analysis of opacity as a function of the impedance.[135] B) Single-cell isolation platform for improved accessibility of single-cell analysis in microbiological research. The different steps are represented: i) cell encapsulation, ii) single-cell droplet sorting, and iii) droplet export. After the encapsulation of single cells, they were analyzed, and iv) bioanalyzer electropherograms were used to demonstrate the size distribution of cDNA molecules.[136] C) Application of microfluidics in the treatment of human infertility: i) microfluidic chip for sperm sorting, and ii) test of sperm viability and fertilization potential.[137] D) On solo-MFP for the ii) growth of follicles and, after hCG stimulation, iii) the finalization of the first meiotic division was achieved as can be seen by the well-organized microtubule fibers (represented in green), well-aligned chromosomes (blue), and the rounded appearance of F-actin (red).[133]

Table 2 Examples of microfluidics in clinical pathology

	Objective	Method
Hematology	Analyze up to 1 million cells per second	256 parallel channels[145]
	Enumerate red blood cells (RBCs), white blood cells (WBCs) and platelets	11-Layer chip using two approaches in parallel: (1) diluting the blood and (2) lysing the RBCs, and then discriminate using an impedance cytometer[135] (Fig. 8a)
	Analyze multiple samples in a single chip	Spinning-disc system based on the different cell densities for cell separation and label-free imaging for analysis[146]
	RBC deformability	- Microfluidic systems able to measure the pressure required for single RBCs to migrate through a micro-constriction[147] - Capacity of stored RBCs to stimulate the production of nitric oxide[148] - Paper-based microfluidic device for RBC transport and haematocrit[149]
	Cell lysis and WBC preparation	A multistep microfluidic on a chip prior to detection by impedance cytometry[150]
	Classification of cell subtypes based on the evaluation of cell size and complexity	Compact lens-free in-line holographic analysis in a microfluidic system[151]
	Leukocyte subgroup classification	Array of leukocyte capture chambers and subsequent analysis using a code-multiplexed Coulter sensor network[152]
	Discriminate neutrophil phenotypes	High-throughput microfluidic optical coulter counter[153]
	Neutrophils analysis with a fingerpick sample of blood	Microfluidic system integrated into a lens-free shadow imaging platform[154]
	Analysis of hemoglobin levels	RBCs driven through a microfluidic channel and analyzed using blue and red LEDs and a microscope[155]
	Diagnose anemia	3D printed microchip using a smartphone by mixing the sample and reagents in a pump-free system fully compatible for low-resource settings or home use[156]
	RBCs separation	High-throughput microfluidic RBC depletion system based on hydrodynamic effects in channel bifurcations[157] and negative dielectrophoresis[158]
	Role of platelets	Microfluidic OvCa-chip that recreated the vascular endothelium in ovarian cancer[159]
Clinical microbiology	Detect the presence of pathogens and classify the species	Separation using different pressure values (i.e. different regions of the microchannel) and monitoring the phenotypic growth of the trapped bacteria in the presence of antibiotic[160]
	Detection of Malaria	- Cell deformability for separation infected red blood cells with *P. falciparum*[161] - Microfluidic deformability sensor (500 cells per second) with 94% sensitivity and 86% specificity[162] - Dielectrophoresis to isolate infected red blood cells combined with a miniaturized PCR[163] - Paper microfluidics and traditional microscopy[164] - Shear-modulated inertial microfluidic system to enrich and purify malaria parasites from blood[165] - Simple-to-use device that can perform complex separations like a fractionation of leukocytes, erythrocytes, and essentially the parasites[166] - Magnetic[167] and optical means[168] - Droplet-based microfluidics technology for single cell isolation and identification[136,169–171] (Fig. 8b)
Reproductive biology	Prenatal screening for single mutations	- High-throughput isolation of fetal trophoblasts and applying fluorescence *in situ* hybridization (FISH) to confirmed trisomy 21 cases[172] - Isolation of trophoblasts from maternal blood applying microscale vortices that combines inertial and microscale vortices forces[173] - Four-stage device for the isolation of fetal trophoblasts, again based in inertial microfluidics and Dean flow forces[174]
	Selection of sperm	- Motility rate of the sperm in a passive sorting approach using two outlet channels[137] (Fig. 8c) - Sorter that minimizes the sperm damage in comparison with traditional density gradients or swim up methods[175] - Combination of intracytoplasmic sperm injection (ICSI) Petri dish with a microfluidic-based array to select the most viable sperm directly from semen[176]
	In vitro fertilisation	- Multifunctional microfluidic device that allows single oocyte trapping, fertilization, and subsequent embryo culture in a single chip[177] - Human embryo model from pluripotent stem cells in a microfluidic device that allowed to study several different post-implantation milestones on a chip[178] - 3D oviduct culture system on a chip[179]
Histology and Cytology	Process multiple tissue samples in a non-destructive manner	Microfluidic device labeling with fluorescent analogues traditional hematoxylin and eosin, as well as other fluorescent markers[180]
	Immunohistochemistry	- Staining of tissue sections, denominated micro-immunohistochemistry[181] - Microfluidic multiplexed immuno-histochemistry platform for (quantitative) pathological diagnosis[182,183]
	Cytology	- Improved cell smear method through a set of contraction–expansion microchannels, based on label-free, continuous, and size-selective particle separation[184]

Table 2 *(continued)*

Objective	Method
Staining and recovery	- Microfluidic platform with an integrated electrical actuator in the form of a cytological slide[185] - Multi-staining chip using hydrophobic valves with a circular chamber divided into six regions, and the switchable injection ports localized in the center[186] - Microfluidic processing of cytology specimens in combination with magnetic immobilization[187,188] - Robust classification model from cytology-on-a-chip measurements[189] - Single-cell western blotting with cell-size filtration and great cell settling efficiencies[190] - Microfluidic paper-based analytical devices to collect fluids and to detect disease- or physiological-related molecules[191]
Flow cytology	- Automatic staining, imaging, and analysis of single-cells for cytopathology using inertial lift forces arising in microscale laminar fluid flow at finite Reynolds number, to position cells in flow and transfer cells across fluid streams[192]
Haematology, oncohaematology	- High throughput method for single cell analyses for the analysis of the fusion gene in 10 simultaneous samples with 50-fold reduction of reagent use and 10-fold less time[193] - Miniaturised FISH system integrating a nanostructured TiO_2 substrate for the immobilization and analysis of hematopoietic cells from peripheral blood or bone marrow samples[194] - Immobilisation of circulating plasma cells and circulating leukemic cells in microtraps for cytogenetic analysis of translocations and fusion aberrations[195] - Automated FISH towards the detection of chromosomal abnormality in leukemia in 45 minutes[196]
Tissue sections	- A thin Pyrex-silicon microfluidic chamber where a square-wave oscillatory flow was applied[197,198] - Integration of microfluidic FISH system with combined analysis of HER2 protein overexpression to evaluate intratumoral heterogeneity[199] - Non-contact microfluidic scanning probe to localize FISH probes to selected cells in the tissue section[200] - Microfluidic-assisted FISH with hydrodynamic flow patterns producing a colorimetric image that can be read out using bright field microscopy[201]
Circulating Tumour Cells (CTCs)	- Microsieve with 10 μm pores where the CTCs were separated from 3 mL diluted blood samples at a high flow rate of up to 2 mL min^{-1} [202] - Chip displayed 3D microchambers for tumor cell capture and high resolution imaging[203] - Fully automated FISH on-chip system for the assessment of ERBB2 in captured cells from pleural fusion samples[204] - Automated DNA and mRNA analysis using *in situ* FISH[205]
Chromosomal DNA analysis	- Telomere length[206] - Chromosomal aneuploidies analysis for prenatal diagnosis applications[207] - Diagnosis of Alzheimer's disease[208] and malaria[209] - Integrate FISH microfluidics in co-culture systems[210] and in microdroplets,[211] and new tools towards real-time monitoring of FISH kinetics[212]
Immunofluorescence	- Dielectrophoretic microfluidic platform for dengue virus detection[213] - Cancer cells: HER2 expression in breast cancer cells,[214] cholangiocarcinoma cells,[215] lung adenocarcinoma *in situ* mapping of immune cells[216] and circulating tumor cells isolation[217–220] - Immunofluorescence for just capture and immunostaining protocol[221,222]

free as in "freedom" and does not necessarily mean "gratis". Free software is provided under terms that guarantee the freedom of its users to run, adapt, and redistribute the software with or without changes. A free software license such as GNU General Public License (GPL) requires that the same rights be preserved in derivative works created from that property so that the software can never be included in proprietary software products (see also https://www.gnu.org/licenses/copyleft.en.html). The concept of open-source software focuses more on the practical consequences enabled by these licenses, while free software focuses on the philosophy behind it. More information about free and open-source licensing can be found in "Understanding Open Source and Free Software Licensing".[138] In this article, the term FLOSS will refer to both Free/Libre and open-Source Software.

It is often difficult to assess the quality of a FLOSS system for the users. Besides the feature list and the functionality, there are several other criteria that can be used to decide about the adoption of a software system. Some criteria that may be checked during the decision process are:

1) Code availability – for a FLOSS system, the code should be available to download either from the website of the provider or from a software repository. Some widely known

software repositories are *e.g.* https://github.com/, https://about.gitlab.com/ or https://sourceforge.net/.

2) Developer community – who is contributing to the code? One of the main advantages of the FLOSS development process is the power of the community. The work-load is distributed on many shoulders and many eyes detect more errors than two or four. An active developer community is also a good indicator for a sustainable project.

3) User community – who is using the system? Is there feedback from the user community? It is very valuable to have the ability to hear the voice of the users. Is the product user friendly? Does it fit into the workflow? Is it possible to integrate the system with other systems?

4) Activity, maturity, roadmap – is the project active, in sleep mode or dead? Is it a mature product or working in beta-phase? Does the project have a roadmap which outlines the future development?

5) Professional support services – is someone offering professional support services? This is important if adaptation and/or integration of the system is needed. Professional Service Providers, as maintainers and developers, have a deep understanding of the codebase and know quickly where and how to implement new features or how to tailor the system to best fit the organization needs.

6) Programming language and tools – is the programming language well known and widely used or is it exotic? Which tools are being used for programming?

7) Governance/ownership/core development team – who is the main developer or brain behind the system? Is it a one person show or is there a team or a company in charge of the development? Who is governing the software development process? Is it a company, a foundation or a community? These are important indicators to assess the sustainability of the product as well as potential support in case it is needed.

8) Documentation – is there enough documentation to understand the system? Is there a developer guide as well as a user guide available? Is the code well documented?

9) Signs of "provider-lock-in" – some providers use the FLOSS approach to create a user community and "lock-in" the users by *e.g.* charging for update-scripts, not providing necessary documentation or the most interesting features are only available in an enterprise version which is not free.

A short overview of some of the currently available systems is present below.

• SENAITE (https://www.senaite.com/) SENAITE is an open-source Laboratory Information Management System (LIMS) for enterprise environments, especially focused to behave with high speed, excellent performance and good stability. It is based on the BIKA LIMS built on top of the Plone CMS with Python as the main programming language. It is a joint effort of Naralabs (https://naralabs.com, Spain) and Riding Bytes (https://www.ridingbytes.com/about/, Germany). The code is available at GitHub: https://github.com/senaite

• BIKA LIMS (https://www.bikalims.org/) has already nearly 20 years of history. Grown out as a LIMS for the wine

industry, it has evolved over several major releases into SENAITE LIMS.

• OpenELIS (https://www.openelis.org/) (https://openelis-global.org/) The OpenELIS project is governed by the OpenELIS Foundation and targeted at the U.S. market as well as low resource settings in Asia, India and Africa. Some of the features worth noting are: sample entry, results entry, user management and administration, role-based security, reporting, data validation, workplans, patient reports, test catalogs, raw data export, instrument integration, English or French language configuration. A demo is available under: http://openelis-global.org/getting-started/demo/. The code is available at Github: https://github.com/openelisglobal/openelisglobal-core

• BaobabLIMS (https://baobablims.org/) Baobab LIMS was developed by customizing the Bika LIMS software to meet the requirement of biobank best practices for human biobanking. https://pubmed.ncbi.nlm.nih.gov/28375759/

• GNU LIMS (https://www.gnuhealth.org/download.html). GNU LIMS, also known as Occhiolino, is a modern Laboratory Information Management System for the healthcare and biomedical sectors that has emerged as a sub-project of the free/libre health and hospital information management system GNU Health. It is fully integrated into GNU Health. A standalone version will need some customization effort.

In conclusion, there are a couple of FLOSS LIMS available that provide the same or better functionality than proprietary systems. One of the biggest advantages of FLOSS is that it can be adapted to the user needs and extended if a needed interface or functionality is missing. Using the checklist above may help to find out the best fitting system for a particular use.

5. Analytical & clinical validation

The development of open-source and cost-effective technologies facilitates the reproducibility, modifications and improvements by the different users. However, as with any other device, these products should be validated prior to their use. Since validation will be highly-dependent on the technology used and it is similar to commercial technologies, only a brief summary with the main points will be presented here.

From May 2022, all new devices should meet the requirements of the European Regulation (EU) 2017/746 on *in vitro* diagnostic medical devices to be placed in the European market, that establishes more restrictive requirements for IVDs in terms of quality, safety, and reliability.[139] This Regulation includes the need to conduct clinical performance studies, and safety and performance evaluations, as described below. This new regulation entered in force on 25th May 2017 and has a transition period of five years. Therefore, the relative benefits will be clear in the coming years, especially because most of the self-certified IVDs must be re-certified following the IVDR and thus, subjected to conformity assessment by a Notified Body.

In the meantime, the aforementioned WHO Model List of Essential *In Vitro* Diagnostic (EDL) itself is a kind of guarantee of reliability, considering that the criteria for product selection were (a) the usefulness for public health of the test category, as determined, for example, from the disease burden; (b) the validity of commercial IVDs, as confirmed by sound, adequate data on quality, safety, performance and regulatory status; (c) their clinical effectiveness, as confirmed by published, peer-reviewed data on safety and cost-effectiveness; (d) the appropriateness of the IVD category for use at specified levels of the laboratory or health care system; and e) the infrastructure required, target users, sample type and volume, sample handling, time to results, storage conditions, operating conditions, shipping requirements, training and skill requirements, associated equipment, throughput, need for maintenance, disposal and connectivity, as appropriate.[140] Unfortunately, currently the EDL is very short since it prefers the WHO key diseases. However, the EDL will be updated annually and surely represents a starting point to ensure full implementation in clinical pathology laboratories.

Every cost-effective technology has to prove that meets the safety and performance requirements for the user. In this sense, the requirements may vary depending on sample type, technology used, and if the device is designed to be used by specialized personnel, or consists on in-house devices used by the patient. In this sense, it is crucial to consider the particularities of the different analytical techniques during the development and validation processes. For example, in the case of assays in which immunoreactions take place in a very short time, *i.e.* from seconds to two minutes as in LFIA, the antibodies selection should be wary of traditional antibodies evaluation using enzyme linked immunosorbent assay that relies on longer incubation times.

Similarly, the validation of the technology should start during the developing phase to assure accurate and precise results. For example, initially, results from OS or cost-effective devices could be compared against those obtained using commercially available closed-source systems, which were validated prior to their distribution. For this, the same samples could be divided in two aliquots and measured using the cost-effective and the commercial device, which can be considered as the gold-standard if it was previously validated. In a more advanced phase, the devices should be validated as determined by the 2017/746 European Regulation and Guides for Industry[141] or equivalent, which can be summarized as:

• Accuracy of the measurements. This section refers to studies determining the trueness of the measurement if a certified reference material or method is available (which needs to be traceable and replicable for subsequent quality controls, which is not always possible), and the precision of the measurement determined by performing repeatability and reproducibility studies.

• Reproducibility studies and evaluation of possible interferences of potential pre-processing factors that may affect intra- and inter-laboratory reproducibility. Thus, it is highly encouraged to pre-register all experimental designs and analyses and to establish standardized working conditions.

• Diagnostic sensitivity, determining the assay's capacity of detecting positive samples, taking into account the specimen type and sample preparation and analyte levels.

• Diagnostic specificity, determining the assay's capacity of detecting negative samples, considering the possible interference of other endogenous or exogenous substances or cross reactivity studies.

• Assay range, include the limits of detection (the range of values that can be measured precisely), the measuring system (linear or non-linear), if high samples can be diluted, or the presence of Hook effect.

• Assay cut-off, in which the study design is described including data about the studied population, characterization of specimens, and statistical methods employed to generate results (grey-zone/equivocal zone, Receiver Operator Characteristic (ROC), *etc.*).

• Stability and in-use stability, referring to the period of time in which the assay maintained its validation characteristics in at least three different lots in similar conditions of routine production and use. For example, shelf-life of unused product, in-use stability, or stability at different temperatures for POC devices.

In addition, for POC implementation in routine clinical laboratories, the manufacturing process should be reliable enough to assure the same quality across different lots. Besides, an extensive validation at the end-user level should be performed to assess the test performance under real life conditions, considering the respective prevalence of the disease and possible comorbidities, and thus obtaining reliable clinical accuracy data. Last but not least, the long-term quality assurance must be assessed through post-marketing surveillance.

During the development and validation of assays, the pre-processing of raw data such as baseline correction, signal to noise ratio reduction, deconvolution of peaks, scaling, centering, and transformations for the multitude signals is essential. For this, novel approaches such as Machine Learning and Artificial Intelligence facilitates the categorization of samples using algorithms based on target analyte, noise reduction, improved specificity and recognition, direct and fast readout, as well as improved reliability. In addition, other possible ways for validation include mathematical models, characteristics of printed materials and simulations.

OS software should be also validated. For example, for image analysis tools, the same images can be acquired and quantified with the cost-effective tool and with a widely used and validated software package.[142] There are also prerequisites for software verification and validation in the European Regulation, requesting for evidence of the software validation in its finished device. This typically includes information about hardware configuration and operating

systems, as well as results from verification, validation and performance in the user environment.

Last, it would be extremely helpful if manufacturers would not only focus on the technical performance aspects, but also provide information regarding clinical utility, clinical risk management, and health economical aspects (*i.e.*, the quantification of health and economic impact through the comparative analysis of alternative courses of action[143]). Data resulting from cost–benefit, cost-effectiveness and cost-utility analysis are priceless to the healthcare system decision makers, although, currently, a large portion of commercially available tests does not provide all the aforementioned information. In this regard, Kosack *et al.*[144] outlined a six-step guide that may help clinics, laboratories, and health ministries to the selection and implementation of IVD tests based on Médecins sans frontiers practical experience: (1) define the test's purpose; (2) review the market; (3) ascertain regulatory approval; (4) determine the test's diagnostic accuracy under ideal conditions; (5) determine the test's diagnostic accuracy in clinical practice; (6) monitor the test's performance in routine use. However, since the evaluation process requires a lot of work and time, it can easily lead the end user to desist, even if interested in the implementation.

Overall, after a correct validation, cost-effective technologies can be efficiently employed, leading to more affordable alternatives or complements to commercial software, methods or instruments; or even, in some cases, the only way of performing some assays.

Summary and conclusions

In conclusion, this review showed the potential of different cost-effective alternatives for the routine clinical pathology laboratory. The inclusion of the OS approach can markedly improve clinical pathology laboratories by introducing new different technologies resulting in faster, more economic, efficient and suitable solutions.

These technologies allow significantly reducing the costs for clinical pathology laboratories in terms of equipment, processing or specialized personnel compared to conventional approaches. 3D printing technology has proved to be a valuable approach for building simple DIY lab equipment at significantly lower costs than similar equipment commercially available and allowing high customization of designs. A wide variety of POCT has power to identify, detect and monitor changes in organisms with a series of advantages compared to traditional methods including economic savings, anyplace and real-time monitoring, do not need specific instruments nor personnel, and low sample volume. And there is a variety of FLOSS that can be adapted to the user needs and constituted feasible alternatives to proprietary digital tools.

Overall, it is expected that these tools will continue evolving in the next years, contributing to cost-effective assays that would further extend the set of clinical pathology

test suitable for use inside and outside the laboratories, making it more accessible worldwide.

Conflicts of interest

The authors declare no conflict of interest.

References

1 P. Bankhead, M. B. Loughrey, J. A. Fernández, Y. Dombrowski, D. G. McArt, P. D. Dunne, S. McQuaid, R. T. Gray, L. J. Murray, H. G. Coleman, J. A. James, M. Salto-Tellez and P. W. Hamilton, *Sci. Rep.*, 2017, **7**(1), DOI: 10.1038/s41598-017-17204-5.

2 J. M. Pearce, *Inventions*, 2018, **3**, 44.

3 B. Wijnen, E. J. Hunt, G. C. Anzalone and J. M. Pearce, *PLoS One*, 2014, **9**(9), DOI: 10.1371/journal.pone.0107216.

4 T. Baden, A. M. Chagas, G. Gage, T. Marzullo, L. L. Prieto-Godino and T. Euler, *PLoS Biol.*, 2015, **13**, e1002086.

5 J. M. Pearce, *HardwareX*, 2020, **8**, e00139.

6 R. Craig, J. P. Cortens and R. C. Beavis, *J. Proteome Res.*, 2004, **3**, 1234–1242.

7 C. DiBona, S. Ockman and M. Stone, *Comput. Math. with Appl.*, 1999, **37**, 173.

8 B. G. L. Nelissen, J. A. van Herwaarden, F. L. Moll, P. J. van Diest and G. Pasterkamp, *PLoS One*, 2014, **9**, e110289.

9 World Health Organization, *First WHO Model List of Essential In Vitro Diagnostics*, Geneva, 2019.

10 United Nations, *Transforming our World: The 2030 Agenda for Sustainable Development | Department of Economic and Social Affairs*, 2015.

11 A. Silver, *Nature*, 2019, **565**, 123–124.

12 M. Coakley and D. E. Hurt, *J. Lab. Autom.*, 2016, **21**, 489–495.

13 *Adjustable Volume Straw Pipette by kwalus*, https://www.thingiverse.com/thing:64977, (accessed 18 February 2021).

14 *Adjustable Volume Straw Pipette (simpler plunger) by aliekens*, https://www.thingiverse.com/thing:74502, (accessed 18 February 2021).

15 *Laboratory Pipette by lewisite*, https://www.thingiverse.com/thing:159052, (accessed 18 February 2021).

16 *Biropette: customisable, high precision pipette by BadenLab*, https://www.thingiverse.com/thing:255519, (accessed 22 February 2021).

17 *Seiken's laboratory micropipette by hermitwhite*, https://www.thingiverse.com/thing:2413630, (accessed 22 February 2021).

18 J. Bravo-Martinez, *HardwareX*, 2018, **3**, 110–116.

19 M. D. Brennan, F. F. Bokhari and D. T. Eddington, *Micromachines*, 2018, **9**, 191.

20 *The DeRisi Lab, Pipet Rack*, http://derisilab.ucsf.edu/index.php?3D=92, (accessed 23 February 2021).

21 *Rack for Biropettes*, Customizable by BadenLab, https://www.thingiverse.com/thing:257254, (accessed 23 February 2021).

22 *Magnetic Rack for 8*, 1.5mL Tubes by acadey, https://www.thingiverse.com/thing:79424, (accessed 23 February 2021).

23 *F.Lab's Tube Rack Blocks by F_Lab_TH*, https://www.thingiverse.com/thing:1175428, (accessed 18 February 2021).

24 *3D Printable Lab test tube holder by Aigars Inserts*, https://www.myminifactory.com/object/3d-print-lab-test-tube-holder-34669, (accessed 23 February 2021).

25 *Test Tube Rack by mtvasuvius*, https://www.thingiverse.com/thing:2269868, (accessed 23 February 2021).

26 *Parametric Test Tube / Centrifuge Tube Rack by JediJeremy*, https://www.thingiverse.com/thing:3147311, (accessed 23 February 2021).

27 *Tube Rack | NIH 3D Print Exchange*, https://3dprint.nih.gov/discover/3dpx-000490, (accessed 23 February 2021).

28 *1.5ml tube rack, holds 49 tubes by DownloadableLabs*, https://www.thingiverse.com/thing:4795054, (accessed 27 March 2021).

29 *Petri Dish Rack, 9 x 90mm Plates by JonoRig*, https://www.thingiverse.com/thing:3105122 (accessed 23 February 2021).

30 *3D Printable Lab bench vial holders by Jeff Crews*, https://www.myminifactory.com/object/3d-print-lab-bench-vial-holders-22453, (accessed 23 February 2021).

31 T. H. Lücking, F. Sambale, B. Schnaars, D. Bulnes-Abundis, S. Beutel and T. Scheper, *Eng. Life Sci.*, 2015, **15**, 57–64.

32 D. Zielinski, A. Gordon, B. L. Zaks and Y. Erlich, *Nat. Methods*, 2014, **11**, 784–785.

33 *Oriceps*, https://www.thingiverse.com/thing:2988740, (accessed 23 February 2021).

34 *Cross tweezer by joo*, https://www.thingiverse.com/thing:25587, (accessed 18 February 2021).

35 T. R. Damase, D. Stephens, A. Spencer and P. B. Allen, *J. Biol. Methods*, 2015, **2**, e24.

36 *Customizable Gel Comb by anoved*, https://www.thingiverse.com/thing:352873, (accessed 24 February 2021).

37 L. Raddatz, I. de Vries, J. Austerjost, A. Lavrentieva, D. Geier, T. Becker, S. Beutel and T. Scheper, *Eng. Life Sci.*, 2017, **17**, 931–939.

38 *Greiner 1536 PP Microplate Flange Replacement | NIH 3D Print Exchange*, https://3dprint.nih.gov/discover/3DPX-000368, (accessed 18 February 2021).

39 *Coverslip spinner holder | NIH 3D Print Exchange*, https://3dprint.nih.gov/discover/3dpx-001230, (accessed 18 February 2021).

40 D. K. Trivedi and J. M. Pearce, *Appl. Sci.*, 2017, **7**, 942.

41 *Corning Cell Culture Plate Holder by AMickle*, https://www.thingiverse.com/thing:4360834, (accessed 23 February 2021).

42 K. C. Dhankani and J. M. Pearce, *HardwareX*, 2017, **1**, 1–12.

43 *DIYbio Centrifuge V 3.0 by ProgressTH*, https://www.thingiverse.com/thing:3702648, (accessed 23 February 2021).

44 *3D Printed DIYbio Mini-Centrifuge : 5 Steps - Instructables*, https://www.instructables.com/3D-Printed-DIYbio-Mini-Centrifuge/, (accessed 2 April 2021).

45 *DremelFuge - A One-Piece Centrifuge for Rotary Tools by cathalgarvey*, https://www.thingiverse.com/thing:1483, (accessed 23 February 2021).

46 F. Lab, *F.Lab's DIYbio Magnetic Stirrer by F_Lab_TH - Thingiverse*, https://www.thingiverse.com/thing:1175415, (accessed 2 April 2021).

47 *Magnetic stirrer from a 80 mm fan by WaveSupportApparatus*, https://www.thingiverse.com/thing:1663540, (accessed 23 February 2021).

48 A. Jönsson, A. Toppi and M. Dufva, *HardwareX*, 2020, **8**, e00115.

49 *Microscope Stand by Perinski*, https://www.thingiverse.com/thing:3379567, (accessed 24 February 2021).

50 *3D Printed USB Microscope Stand by PrintableScience*, https://www.thingiverse.com/thing:2993860, (accessed 18 February 2021).

51 *A Fully Printable Microscope by kwalus*, https://www.thingiverse.com/thing:77450, (accessed 18 February 2021).

52 *A Printable Microscope Smartphone Adapter by kwalus*, https://www.thingiverse.com/thing:92355, (accessed 24 February 2021).

53 *OpenSCAD smart phone to microscope/telescope adapter by Boogie*, https://www.thingiverse.com/thing:231265, (accessed 24 February 2021).

54 *PNNL Smartphone Microscope - Available Technologies - PNNL*, https://availabletechnologies.pnnl.gov/technology.asp?id=393, (accessed 24 February 2021).

55 *The Public Lab: Spectrometry*, https://publiclab.org/wiki/spectrometry, (accessed 2 April 2021).

56 *Modular Spectrometer by ndamrauer*, https://www.thingiverse.com/thing:4566453, (accessed 24 February 2021).

57 K. Laganovska, A. Zolotarjovs, M. Vázquez, K. Mc Donnell, J. Liepins, H. Ben-Yoav, V. Karitans and K. Smits, *HardwareX*, 2020, **7**, e00108.

58 M. D. Brennan, M. L. Rexius-Hall and D. T. Eddington, *PLoS One*, 2015, **10**, e0137631.

59 J. Wu, M. Dong, C. Rigatto, Y. Liu and F. Lin, *NPJ Digit. Med.*, 2018, **1**, 1–11.

60 N. Kolluri, C. M. Klapperich and M. Cabodi, *Lab Chip*, 2018, **18**, 75–94.

61 J. Wu, M. Dong, S. Santos, C. Rigatto, Y. Liu and F. Lin, *Sensors*, 2017, **17**(12), DOI: 10.3390/s17122934.

62 S. Ketterer, D. Hövermann, R. J. Guebeli, F. Bartels-Burgahn, D. Riewe, T. Altmann, M. D. Zurbriggen, B. Junker, W. Weber and M. Meier, *Anal. Chem.*, 2014, **86**, 12152–12158.

63 A. H. C. Ng, R. Fobel, C. Fobel, J. Lamanna, D. G. Rackus, A. Summers, C. Dixon, M. D. M. Dryden, C. Lam, M. Ho, N. S. Mufti, V. Lee, M. A. M. Asri, E. A. Sykes, M. D. Chamberlain, R. Joseph, M. Ope, H. M. Scobie, A. Knipes, P. A. Rota, N. Marano, P. M. Chege, M. Njuguna, R. Nzunza, N. Kisangau, J. Kiogora, M. Karuingi, J. W. Burton, P. Borus, E. Lam and A. R. Wheeler, *Sci. Transl. Med.*, 2018, **10**, 1–13.

64 Z. Zhao, H. Cui, W. Song, X. Ru, W. Zhou and X. Yu, bioRxiv, 2020, p. 518055.

65 J. Eills, W. Hale, M. Sharma, M. Rossetto, M. H. Levitt and M. Utz, *J. Am. Chem. Soc.*, 2019, **141**, 9955–9963.

66 C. Zhang, Y. Su, S. Hu, K. Jin, Y. Jie, W. Li, A. Nathan and H. Ma, *ACS Omega*, 2020, **5**(10), 5098–5104.

67 S. Mukherji and D. Mondal, in *Medical Biosensors for Point of Care (POC) Applications*, Elsevier, 2017, pp. 99–131.

68 *Lateral Flow Assay Market Size, Share | Global Industry Report, 2026*, https://www.verifiedmarketresearch.com/product/lateral-flow-assay-market/, (accessed 18 March 2021).

69 W. Han and J. H. Shin, *HardwareX*, 2021, **9**, e00188.

70 S. Choi, J. H. Lee, J. S. Choi and H. Il Jung, *Anal. Methods*, 2015, **7**, 1834–1842.

71 J. Credou, R. Faddoul and T. Berthelot, *RSC Adv.*, 2015, **5**, 29786–29798.

72 D. Wild, R. John and C. Sheehan, in *The Immunoassay Handbook*, ed. D. Wild, Elsevier Science, 4th edn, 2013, pp. 109–121.

73 World Health Organization, *Second WHO Model List of Essential In Vitro Diagnostics*, 2019.

74 M. Zangheri, F. Di Nardo, D. Calabria, E. Marchegiani, L. Anfossi, M. Guardigli, M. Mirasoli, C. Baggiani and A. Roda, *Anal. Chim. Acta*, 2021, **1163**, 338515.

75 S. Ghosh, K. Aggarwal, T. U. Vinitha, T. Nguyen, J. Han and C. H. Ahn, *Microsyst. Nanoeng.*, 2020, **6**(1), DOI: 10.1038/s41378-019-0108-8.

76 M. Zangheri, L. Cevenini, L. Anfossi, C. Baggiani, P. Simoni, F. Di Nardo and A. Roda, *Biosens. Bioelectron.*, 2015, **64**, 63–68.

77 S. Parra, E. Carranza, J. Coole, B. Hunt, C. Smith, P. Keahey, M. Maza, K. Schmeler and R. Richards-Kortum, *IEEE J. Transl. Eng. Health Med.*, 2020, **8**, DOI: 10.1109/JTEHM.2020.2970694.

78 A. Huttunen, S. Aikio, M. Kurkinen, J. T. Mäkinen, R. Mitikka, L. Kivimäki, M. Harjumaa, J. Takalo-Mattila, C. Liedert, J. Hiltunen and L. Hakalahti, *IEEE Sens. J.*, 2020, **20**, 10275–10282.

79 L. J. Wang, R. Sun, T. Vasile, Y. C. Chang and L. Li, *Anal. Chem.*, 2016, **88**, 8302–8308.

80 J. Jiang, X. Wang, S. Li, F. Ding, N. Li, S. Meng, R. Li, J. Qi, Q. Liu and G. L. Liu, *Nanophotonics*, 2018, **7**, 1517–1531.

81 S. M. Fothergill, C. Joyce and F. Xie, *Nanoscale*, 2018, **10**, 20914–20929.

82 J. Satija, N. Punjabi, D. Mishra and S. Mukherji, *RSC Adv.*, 2016, **6**, 85440–85456.

83 R. De La Rica and M. M. Stevens, *Nat. Nanotechnol.*, 2012, **7**, 821–824.

84 C. D. Geddes and J. R. Lakowicz, *J. Fluoresc.*, 2002, **12**, 121–129.

85 M. Li, S. K. Cushing and N. Wu, *Analyst*, 2015, **140**, 386–406.

86 R. Knoblauch and C. D. Geddes, in *Reviews in Plasmonics*, ed. C. D. Geddes, Springer International Publishing, Cham, 2019, vol. 2017, pp. 253–283.

87 J. Waitumbi, G. Awinda, G.-H. Rajasekariah, C. Kifude and S. K. Martin, *Am. J. Trop. Med. Hyg.*, 2009, **80**, 516–522.

88 A. Minopoli, *et al.*, *Microchim. Acta*, 2021, **188**, 88.

89 A. Minopoli, B. Della Ventura, B. Lenyk, F. Gentile, J. A. Tanner, A. Offenhäusser, D. Mayer and R. Velotta, *Nat. Commun.*, 2020, **11**, 6134.

90 B. Della Ventura, M. Banchelli, R. Funari, A. Illiano, M. De Angelis, P. Taroni, A. Amoresano, P. Matteini and R. Velotta, *Analyst*, 2019, **144**, 6871–6880.

91 G. Guglielmi, *Nature*, 2020, **583**, 506–509.

92 S. A. Bustin and R. Mueller, *Clin. Sci.*, 2005, **109**, 365–379.

93 S. Olofsson, R. Brittain-Long, L. M. Andersson, J. Westin and M. Lindh, *Expert Rev. Anti-infect. Ther.*, 2011, **9**, 615–626.

94 Ö. Appak, M. Duman, N. Belet and A. A. Sayiner, *J. Med. Virol.*, 2019, **91**, 731–737.

95 M. Satyanarayana, Shortage of RNA Extraction Kits Hampers Efforts to Ramp up COVID-19 Coronavirus Testing, *Chem. Eng. News*, 2020, ISSN 0009-2347.

96 B. Della Ventura, M. Cennamo, A. Minopoli, R. Campanile, S. B. Censi, D. Terracciano, G. Portella and R. Velotta, *ACS Sens.*, 2020, **5**, 3043–3048.

97 Y. Liu, L. Zhang, W. Wei, H. Zhao, Z. Zhou, Y. Zhang and S. Liu, *Analyst*, 2015, **140**, 3989–3995.

98 J. El-Ali, P. K. Sorger and K. F. Jensen, *Nature*, 2006, **442**, 403–411.

99 P. Yager, T. Edwards, E. Fu, K. Helton, K. Nelson, M. R. Tam and B. H. Weigl, *Nature*, 2006, **442**, 412–418.

100 J. Sun, M. Masterman-Smith, N. A. Graham, J. Jiao, J. Mottahedeh, D. R. Laks, M. Ohashi, J. Dejesus, K. Kamei, K. Lee, H. Wang, Z. F. Yu, Y.-T. Lu, S. Hou, K. Li, M. Liu, N. Zhang, S. Wang, B. Angénieux, E. Panosyan, E. R. Samuels, J. Park, D. Williams, V. Konkankit, D. Nathanson, R. M. van Dam, M. Phelps, H. Wu, L. Liau, P. Mischel, J. Lazareff, H. Kornblum, W. Yong, T. Graeber and H. Tseng, *Cancer Res.*, 2010, **70**(15), 6128–6138.

101 N. M. Fuad, M. Carve, J. Kaslin and D. Wlodkowic, *Micromachines*, 2018, **9**, 1–11.

102 F. Perdigones and J. M. Quero, *Sens. Actuators, A*, 2019, **300**, 111639.

103 G. S. Monfared, P. Ertl and M. Rothbauer, *Sci. Rep.*, 2020, **10**, 1–14.

104 L. Cao, G. C. Han, H. Xiao, Z. Chen and C. Fang, *Anal. Chim. Acta*, 2020, **1096**, 34–43.

105 T. U. Vinitha, S. Ghosh, A. Milleman, T. Nguyen and C. H. Ahn, *Lab Chip*, 2020, **20**, 1961–1974.

106 M. A. Messina, C. Meli, S. Conoci and S. Petralia, *Analyst*, 2017, **142**, 4629–4632.

107 E. L. Rossini, M. I. Milani, E. Carrilho, L. Pezza and H. R. Pezza, *Anal. Chim. Acta*, 2018, **997**, 16–23.

108 D. G. Jung, D. Jung and S. H. Kong, *Sensors*, 2017, **17**, 1–12.

109 A. Martín, J. Kim, J. F. Kurniawan, J. R. Sempionatto, J. R. Moreto, G. Tang, A. S. Campbell, A. Shin, M. Y. Lee, X. Liu and J. Wang, *ACS Sens.*, 2020, **3**, 48.

110 A. Chiadò, G. Palmara, A. Chiappone, C. Tanzanu, C. F. Pirri, I. Roppolo and F. Frascella, *Lab Chip*, 2020, **20**, 665–674.

111 S. R. Balakrishnan, U. Hashim, S. C. B. Gopinath, P. Poopalan, H. R. Ramayya, M. I. Omar, R. Haarindraprasad and P. Veeradasan, *PLoS One*, 2015, **10**, 1–17.

112 K. Kadimisetty, A. P. Spak, K. S. Bhalerao, M. Sharafeldin, I. M. Mosa, N. H. Lee and J. F. Rusling, *Anal. Methods*, 2018, **10**, 4000–4006.

113 K. Kadimisetty, S. Malla, K. S. Bhalerao, I. M. Mosa, S. Bhakta, N. H. Lee and J. F. Rusling, *Anal. Chem.*, 2018, **90**, 7569–7577.

114 K. Kaarj, P. Akarapipad and J. Y. Yoon, *Sci. Rep.*, 2018, **8**, 1–11.

115 X. Cai, H. Zhang, X. Yu and W. Wang, *Talanta*, 2020, **216**, 120996.

116 G. G. Nestorova, B. S. Adapa, V. L. Kopparthy and E. J. Guilbeau, *Sens. Actuators, B*, 2016, **225**, 174–180.

117 G. D. Kaprou, G. Papadakis, D. P. Papageorgiou, G. Kokkoris, V. Papadopoulos, I. Kefala, E. Gizeli and A. Tserepi, *Microsyst. Technol.*, 2016, **22**, 1529–1534.

118 H. Haick and N. Tang, *ACS Nano*, 2021, **15**(3), 3557–3567.

119 F. Cui, Y. Yue, Y. Zhang, Z. Zhang and H. S. Zhou, *ACS Sens.*, 2020, **5**, 3346–3364.

120 N. Castaño, S. C. Cordts, K. C. Nadeau, M. Tsai, S. J. Galli and S. K. Y. Tang, *Biomicrofluidics*, 2020, **14**, 21503.

121 L. Gervais, N. de Rooij and E. Delamarche, *Adv. Mater.*, 2011, **23**, H151–H176.

122 G. E. Imade, B. Badung, S. Pam, O. Agbaji, D. Egah, A. S. Sagay, J.-L. Sankalé, S. Kapiga, J. Idoko and P. Kanki, *Clin. Diagn. Lab. Immunol.*, 2005, **12**, 224.

123 C. Lopes, P. Piairo, A. Chícharo, S. Abalde-Cela, L. R. Pires, P. Corredeira, P. Alves, L. Muinelo-Romay, L. Costa and L. Diéguez, *Cancers*, 2021, **13**, 4446.

124 L. Gorgannezhad, H. Stratton and N.-T. Nguyen, *Micromachines*, 2019, **10**, 408.

125 X. Feng, B.-F. Liu, J. Li and X. Liu, *Mass Spectrom. Rev.*, 2015, **34**, 535–557.

126 W. Jing, W. Zhao, S. Liu, L. Li, C.-T. Tsai, X. Fan, W. Wu, J. Li, X. Yang and G. Sui, *Anal. Chem.*, 2013, **85**, 5255–5262.

127 M. Al-Adhami, D. Tilahun, G. Rao, C. Gurramkonda and Y. Kostov, *Methods Mol. Biol.*, 2017, **1571**, 287–299.

128 Z. Altintas, M. Akgun, G. Kokturk and Y. Uludag, *Biosens. Bioelectron.*, 2018, **100**, 541–548.

129 C.-H. Wang, K.-Y. Lien, T.-Y. Wang, T.-Y. Chen and G.-B. Lee, *Biosens. Bioelectron.*, 2011, **26**, 2045–2052.

130 T. Notomi, Y. Mori, N. Tomita and H. Kanda, *J. Microbiol.*, 2015, **53**, 1–5.

131 A. Nikshad, A. Aghlmandi, R. Safaralizadeh, L. Aghebati-Maleki, M. E. Warkiani, F. M. Khiavi and M. Yousefi, *Life Sci.*, 2021, **265**, 118767.

132 N. Kashaninejad, M. J. A. Shiddiky and N.-T. Nguyen, *Adv. Biosyst.*, 2018, **2**, 1700197.

133 S. Xiao, J. R. Coppeta, H. B. Rogers, B. C. Isenberg, J. Zhu, S. A. Olalekan, K. E. McKinnon, D. Dokic, A. S. Rashedi, D. J. Haisenleder, S. S. Malpani, C. A. Arnold-Murray, K. Chen, M. Jiang, L. Bai, C. T. Nguyen, J. Zhang, M. M. Laronda, T. J. Hope, K. P. Maniar, M. E. Pavone, M. J. Avram, E. C. Sefton, S. Getsios, J. E. Burdette, J. J. Kim, J. T. Borenstein and T. K. Woodruff, *Nat. Commun.*, 2017, **8**, 1–13.

134 S. M. Hattersley, C. E. Dyer, J. Greenman and S. J. Haswell, *Lab Chip*, 2008, **8**, 1842–1846.

135 U. Abbasi, P. Chowdhury, S. Subramaniam, P. Jain, N. Muthe, F. Sheikh, S. Banerjee and V. Kumaran, *Sci. Rep.*, 2019, **9**, 18583.

136 Q. Zhang, T. Wang, Q. Zhou, P. Zhang, Y. Gong, H. Gou, J. Xu and B. Ma, *Sci. Rep.*, 2017, **7**, 41192.

137 C. Phiphattanaphiphop, K. Leksakul, R. Phatthanakun and T. Khamlor, *Sci. Rep.*, 2020, **10**, 1–13.

138 A. M. S. St. Laurent, *Understanding Open Source and Free Software Licensing*, 2004.

139 The European Parliament and the Council of the European Union, *Regulation (EU) 2017/746 of the European Parliament and of the Council of 5 April 2017 on in vitro diagnostic medical devices and repealing Directive 98/79/EC and Commission Decision 2010/227/EU*, 2017.

140 World Health Organization, *The selection and use of essential in vitro diagnostics: report of the second meeting of the WHO Strategic Advisory Group of Experts on In Vitro Diagnostics (including the second WHO model list of essential in vitro diagnostics)*, 2019.

141 Food and Drug Administration U.S., *Bioanalytical Method Validation*, U.S. Department of Health and Human Services Food and Drug Administration, 2018, pp. 1–41.

142 P. M. Gordaliza, J. M. Mateos-Pérez, P. Montesinos, J. A. Guzmán-de-Villoria, M. Desco and J. J. Vaquero, *Comput. Biol. Med.*, 2015, **58**, 56–62.

143 M. Drummond, A. Griffin and R. Tarricone, *Value Health*, 2009, **12**, 402–404.

144 C. S. Kosack, A. L. Page and P. R. Klatser, *Bull. W. H. O.*, 2017, **95**, 639–645.

145 S. C. Hur, H. T. K. Tse and D. Di Carlo, *Lab Chip*, 2010, **10**, 274–280.

146 R. Agarwal, A. Sarkar, A. Bhowmik, D. Mukherjee and S. Chakraborty, *Biosens. Bioelectron.*, 2020, **150**, 111935.

147 K. Matthews, M. E. Myrand-Lapierre, R. R. Ang, S. P. Duffy, M. D. Scott and H. Ma, *J. Biomech.*, 2015, **48**, 4065–4072.

148 Y. Wang, A. Giebink and D. M. Spence, *Integr. Biol.*, 2014, **6**, 65–75.

149 S. B. Berry, S. C. Fernandes, A. Rajaratnam, N. S. Dechiara and C. R. Mace, *Lab Chip*, 2016, **16**, 3689–3694.

150 X. Han, C. van Berkel, J. Gwyer, L. Capretto and H. Morgan, *Anal. Chem.*, 2012, **84**, 1070–1075.

151 D. Vercruysse, A. Dusa, R. Stahl, G. Vanmeerbeeck, K. De Wijs, C. Liu, D. Prodanov, P. Peumans and L. Lagae, *Lab Chip*, 2015, **15**, 1123–1132.

152 R. Liu, A. K. M. Arifuzzman, N. Wang, O. Civelekoglu and A. F. Sarioglu, *J. Microelectromech. Syst.*, 2020, **29**, 942–947.

153 E. Schonbrun and G. Di Caprio, *J. Biomed. Opt.*, 2015, **20**, 111205.

154 H. Inan, J. L. Kingsley, M. O. Ozen, H. C. Tekin, C. R. Hoerner, Y. Imae, T. J. Metzner, J. S. Preiss, N. G. Durmus, M. Ozsoz, H. Wakelee, A. C. Fan, E. Tüzel and U. Demirci, *Small Methods*, 2017, **1**, 1700193.

155 E. Schonbrun, R. Malka, G. Di Caprio, D. Schaak and J. M. Higgins, *Cytometry, Part A*, 2014, **85**, 332–338.

156 K. Plevniak, M. Campbell, T. Myers, A. Hodges and M. He, *Biomicrofluidics*, 2016, **10**, 054113.

157 W. Zhao, T. Zhu, R. Cheng, Y. Liu, J. He, H. Qiu, L. Wang, T. Nagy, T. D. Querec, E. R. Unger and L. Mao, *Adv. Funct. Mater.*, 2016, **26**, 3990–3998.

158 T. Yasukawa, J. Yamada, H. Shiku, T. Matsue and M. Suzuki, *Micromachines*, 2020, 11.

159 B. Saha, T. Mathur, K. F. Handley, W. Hu, V. Afshar-Kharghan, A. K. Sood and A. Jain, *Blood Adv.*, 2020, **4**, 3329–3342.

160 H. Li, P. Torab, K. E. Mach, C. Surrette, M. R. England, D. W. Craft, N. J. Thomas, J. C. Liao, C. Puleo and P. K. Wong, *Proc. Natl. Acad. Sci. U. S. A.*, 2019, **116**, 10270–10279.

161 H. W. Hou, A. A. S. Bhagat, A. G. Lin Chong, P. Mao, K. S. Wei Tan, J. Han and C. T. Lim, *Lab Chip*, 2010, **10**, 2605–2613.

162 X. Yang, Z. Chen, J. Miao, L. Cui and W. Guan, *Biosens. Bioelectron.*, 2017, **98**, 408–414.

163 P. Gascoyne, J. Satayavivad and M. Ruchirawat, *Acta Trop.*, 2004, **89**, 357–369.

164 M. P. Horning, C. B. Delahunt, S. R. Singh, S. H. Garing and K. P. Nichols, *Lab Chip*, 2014, **14**, 2040–2046.

165 M. E. Warkiani, A. K. P. Tay, B. L. Khoo, X. Xiaofeng, J. Han and C. T. Lim, *Lab Chip*, 2015, **15**, 1101–1109.

166 D. Holmes, G. Whyte, J. Bailey, N. Vergara-Irigaray, A. Ekpenyong, J. Guck and T. Duke, *Interface Focus*, 2014, **4**(6), DOI: 10.1098/rsfs.2014.0011.

167 J. Nam, H. Huang, H. Lim, C. Lim and S. Shin, *Anal. Chem.*, 2013, **85**, 7316–7323.

168 S. A. Lee, R. Leitao, G. Zheng, S. Yang, A. Rodriguez and C. Yang, *PLoS One*, 2011, **6**, e26127.

169 A. B. Theberge, F. Courtois, Y. Schaerli, M. Fischlechner, C. Abell, F. Hollfelder and W. T. S. Huck, *Angew. Chem., Int. Ed.*, 2010, **49**, 5846–5868.

170 J. B. Harmon, H. K. Gray, C. C. Young and K. J. Schwab, *PLoS One*, 2020, **15**, e0233239.

171 T. S. Kaminski, O. Scheler and P. Garstecki, *Lab Chip*, 2016, **16**, 2168–2187.

172 M. Winter, T. Hardy, M. Rezaei, V. Nguyen, D. Zander-Fox, M. E. Warkiani and B. Thierry, *Adv. Mater. Technol.*, 2018, **3**, 1800066.

173 A. Vander Plaetsen, J. Weymaere, O. Tytgat, M. Buyle, D. Deforce and F. Van Nieuwerburgh, *Prenatal Diagn.*, 2021, **41**(9), DOI: 10.1002/pd.5901.

174 Y. Huang, S. Yu, S. Chao, L. Wu, M. Tao, B. Situ, X. Ye, Y. Zhang, S. Luo, W. Chen, X. Jiang, G. Guan and L. Zheng, *Lab Chip*, 2020, **20**, 4342–4348.

175 K. Shirota, F. Yotsumoto, H. Itoh, H. Obama, N. Hidaka, K. Nakajima and S. Miyamoto, *Fertil. Steril.*, 2016, **105**, 315–321.e1.

176 S. Xiao, J. Riordon, M. Simchi, A. Lagunov, T. Hannam, K. Jarvi, R. Nosrati and D. Sinton, *Lab Chip*, 2021, **21**, 775–783.

177 S. L. Angione, N. Oulhen, L. M. Brayboy, A. Tripathi and G. M. Wessel, *Fertil. Steril.*, 2015, **103**, 281–290.e5.

178 Y. Zheng, Y. Shao and J. Fu, *Nat. Protoc.*, 2021, **16**, 309–326.

179 M. A. M. M. Ferraz, H. H. W. Henning, T. A. E. Stout, P. L. A. M. Vos and B. M. Gadella, *Ann. Biomed. Eng.*, 2017, **45**, 1731–1744.

180 C. Narciso, K. R. Cowdrick, V. Zellmer, T. Brito-Robinson, P. Brodskiy, D. J. Hoelzle, S. Zhang and J. J. Zartman, *Biomicrofluidics*, 2016, **10**, 21101.

181 R. D. Lovchik, G. V. Kaigala, M. Georgiadis and E. Delamarche, *Lab Chip*, 2012, **12**, 1040–1043.

182 M. S. Kim, S. Kwon and J. K. Park, *Methods Mol. Biol.*, 2013, **949**, 349–364.

183 M. S. Kim, T. Kim, S.-Y. Kong, S. Kwon, C. Y. Bae, J. Choi, C. H. Kim, E. S. Lee and J.-K. Park, *PLoS One*, 2010, **5**, e10441.

184 X. Shi, L. Liu, W. Cao, G. Zhu and W. Tan, *Analyst*, 2019, **144**, 5934–5946.

185 M. Jahangiri, S. Khosravi, H. Moghtaderi, M. Ranjbar, H. Abadijoo, S. Sarmadi, N. Izadi-Mood, E. Shirali, P. Hoseinpour, M. Gity, F. Abbasvandi, L. Mohajerzadeh, M. K. Aghdam and M. Abdolahad, *Sens. Actuators, B*, 2019, **297**, 126733.

186 T. H. Lee, J. Bu, J. E. Moon, Y. J. Kim, Y. T. Kang, Y. H. Cho and I. S. Kim, *J. Micromech. Microeng.*, 2017, **27**, 075022.

187 W. Mojica, R. Bassey, F. Chen, B. Hannahoe, P. Sauer, R. Hard and E. P. Furlani, *Cancer Cytopathol.*, 2014, **122**, 59–69.

188 W. D. Mojica and F. Chen, *Cytopathology*, 2015, **26**, 172–177.

189 T. J. Abram, P. N. Floriano, N. Christodoulides, R. James, A. R. Kerr, M. H. Thornhill, S. W. Redding, N. Vigneswaran, P. M. Speight, J. Vick, C. Murdoch, C. Freeman, A. M. Hegarty, K. D'Apice, J. A. Phelan, P. M. Corby, I. Khouly, J. Bouquot, N. M. Demian, Y. E. Weinstock, S. Rowan, C. K. Yeh, H. S. McGuff, F. R. Miller, S. Gaur, K. Karthikeyan, L. Taylor, C. Le, M. Nguyen, H. Talavera, R. Raja, J. Wong and J. T. McDevitt, *Oral Oncol.*, 2016, **60**, 103–111.

190 J. J. Kim, E. Sinkala and A. E. Herr, *Lab Chip*, 2017, **17**, 855–863.

191 J. Y. Cheng, M. J. Feng, C. C. Wu, J. Wang, T. C. Chang and C. M. Cheng, *Anal. Chem.*, 2016, **88**, 7591–7596.

192 A. P. Tan, J. S. Dudani, A. Arshi, R. J. Lee, H. T. K. Tse, D. R. Gossett and D. Di Carlo, *Lab Chip*, 2014, **14**, 522–531.

193 F. Mughal, S. J. Baldock, E. G. Karimiani, N. Telford, N. J. Goddard and P. J. R. Day, *Genes, Chromosomes Cancer*, 2014, **53**, 255–263.

194 A. Zanardi, D. Bandiera, F. Bertolini, C. Corsini, G. Gregato, P. Milani, E. Barborini and R. Carbone, *BioTechniques*, 2010, **49**, 497–504.

195 K. M. Weerakoon-Ratnayake, S. Vaidyanathan, N. Larkey, K. Dathathreya, M. Hu, J. Jose, S. Mog, K. August, A. K. Godwin, M. L. Hupert, M. A. Witek and S. A. Soper, *Cells*, 2020, **9**, 519.

196 C. H. Tai, C. L. Ho, Y. L. Chen, W. L. Chen and G. Bin Lee, in *Microfluidics and Nanofluidics*, Springer, 2013, vol. 15, pp. 745–752.

197 H. T. Nguyen, R. Trouillon, S. Matsuoka, M. Fiche, L. De Leval, B. Bisig and M. A. M. Gijs, *Lab. Invest.*, 2017, **97**, 93–103.

198 H. T. Nguyen, L. N. Dupont, E. A. Cuttaz, A. M. Jean, R. Trouillon and M. A. M. Gijs, *Microelectron. Eng.*, 2018, **189**, 33–38.

199 H. T. Nguyen, D. Migliozzi, B. Bisig, L. de Leval and M. A. M. Gijs, *Lab. Invest.*, 2019, **99**, 722–732.

200 D. Huber and G. V. Kaigala, *Biomicrofluidics*, 2018, **12**, 042212.

201 H. T. Nguyen, L. S. Bernier, A. M. Jean, R. Trouillon and M. A. M. Gijs, *Microelectron. Eng.*, 2017, **183–184**, 52–57.

202 L. S. Lim, M. Hu, M. C. Huang, W. C. Cheong, A. T. L. Gan, X. L. Looi, S. M. Leong, E. S. C. Koay and M. H. Li, *Lab Chip*, 2012, **12**, 4388–4396.

203 G. Mottet, K. Perez-Toralla, E. Tulukcuoglu, F.-C. Bidard, J.-Y. Pierga, I. Draskovic, A. Londono-Vallejo, S. Descroix, L. Malaquin and J. L. Viovy, *Biomicrofluidics*, 2014, **8**, 024109.

204 K. Perez-Toralla, G. Mottet, E. T. Guneri, J. Champ, F. C. Bidard, J. Y. Pierga, J. Klijanienko, I. Draskovic, L. Malaquin, J. L. Viovy and S. Descroix, *Lab Chip*, 2015, **15**, 811–822.

205 P. Gogoi, S. Sepehri, Y. Zhou, M. A. Gorin, C. Paolillo, E. Capoluongo, K. Gleason, A. Payne, B. Boniface, M. Cristofanilli, T. M. Morgan, P. Fortina, K. J. Pienta, K. Handique and Y. Wang, *PLoS One*, 2016, **11**, e0147400.

206 X. Wang, S. I. Takebayashi, E. Bernardin, D. M. Gilbert, R. Chella and J. Guan, *Biomed. Microdevices*, 2012, **14**, 443–451.

207 S. S. Y. Ho, C. Chua, L. Gole, A. Biswas, E. Koay and M. Choolani, *Prenatal Diagn.*, 2012, **32**, 321–328.

208 J. P. Devadhasan, S. Kim and J. An, *J. Biomed. Sci.*, 2011, **18**, 1–11.

209 K. A. Walzer, H. Fradin, L. Y. Emerson, D. L. Corcoran and J.-T. Chi, *PLoS Genet.*, 2019, **15**, e1008506.

210 J. H. Day, T. M. Nicholson, X. Su, T. L. Van Neel, I. Clinton, A. Kothandapani, J. Lee, M. H. Greenberg, J. K. Amory, T. J. Walsh, C. H. Muller, O. E. Franco, C. R. Jefcoate, S. E. Crawford, J. S. Jorgensen and A. B. Theberge, *Lab Chip*, 2020, **20**, 107–119.

211 S. Guo, W. N. Lin, Y. Hu, G. Sun, D. T. Phan and C. H. Chen, *Lab Chip*, 2018, **18**, 1914–1920.

212 N. Ostromohov, D. Huber, M. Bercovici and G. V. Kaigala, *Anal. Chem.*, 2018, **90**, 11470–11477.

213 E. Iswardy, T. C. Tsai, I. F. Cheng, T. C. Ho, G. C. Perng and H. C. Chang, *Biosens. Bioelectron.*, 2017, **95**, 174–180.

214 D. G. Dupouy, A. T. Ciftlik, M. Fiche, D. Heintze, B. Bisig, L. De Leval and M. A. M. Gijs, *Sci. Rep.*, 2016, **6**, 1–10.

215 L. Y. Hung, N. J. Chiang, W. C. Tsai, C. Y. Fu, Y. C. Wang, Y. S. Shan and G. Bin Lee, *Sci. Rep.*, 2017, **7**, 1–10.

216 S. Brajkovic, B. Pelz, M.-G. Procopio, A.-L. Leblond, G. Repond, A. Schaub-Clerigué, D. G. Dupouy and A. Soltermann, *Diagn. Pathol.*, 2018, **13**, 79.

217 S. Abalde-Cela, P. Piairo and L. Diéguez, *Acta Cytol.*, 2019, 1–13.

218 S. Ribeiro-Samy, M. I. Oliveira, T. Pereira-Veiga, L. Muinelo-Romay, S. Carvalho, J. Gaspar, P. P. Freitas, R. López-López, C. Costa and L. Diéguez, *Sci. Rep.*, 2019, **9**, 8032.

219 S. Cotton, D. Ferreira, J. Soares, A. Peixoto, M. Relvas-Santos, R. Azevedo, P. Piairo, L. Diéguez, C. Palmeira, L. Lima, A. M. N. Silva, L. L. Santos and J. A. Ferreira, *Int. J. Mol. Sci.*, 2021, **22**, 1–25.

220 M. Neves, R. Azevedo, L. Lima, M. I. Oliveira, A. Peixoto, D. Ferreira, J. Soares, E. Fernandes, C. Gaiteiro, C. Palmeira, S. Cotton, S. Mereiter, D. Campos, L. P. Afonso, R. Ribeiro, A. Fraga, A. Tavares, H. Mansinho, E. Monteiro, P. A. Videira, P. P. Freitas, C. A. Reis, L. L. Santos, L. Dieguez and J. A. Ferreira, *N. Biotechnol.*, 2019, **49**, DOI: 10.1016/J.NBT.2018.09.004.

221 O. Gagliano, C. Luni, W. Qin, E. Bertin, E. Torchio, S. Galvanin, A. Urciuolo and N. Elvassore, *Nat. Protoc.*, 2019, **14**, 722–737.

222 C. Luni, S. Giulitti, E. Serena, L. Ferrari, A. Zambon, O. Gagliano, G. G. Giobbe, F. Michielin, S. Knöbel, A. Bosio and N. Elvassore, *Nat. Methods*, 2016, **13**, 446–452.